NTNU – Trondheim
Norwegian University of
Science and Technology

Effects of environmental exposure: Interplay between helix-distorting and oxidative DNA lesions and their repair

Solveig Margrethe B. Lakså

Environmental Toxicology and Chemistry

Supervisor: Åse Krøkje, IBI
Co-supervisor: Ann-Karin Hardie Olsen, Nasjonalt folkehelseinstitutt
Kristine Bjerve Gützkow, Nasjonalt

Norwegian University of Science and Technology
Department of Biology

Effects of environmental exposure: Interplay between helix-distorting and oxidative DNA lesions and their repair

Solveig Margrethe Bergseng Lakså

Master's Thesis in Environmental Toxicology

Department of Biology (IBI),
Faculty of Natural Sciences and Technology,
Norwegian University of Science and Technology (NTNU)

In collaboration with:
Department of Chemicals and Radiation (MIKS),
Division of Environmental Medicine,
Norwegian Institute of Public Health (NIPH)

Supervisors:
Associate Professor Åse Krøkje, PhD (IBI, NTNU)
Scientist Ann-Karin H. Olsen, PhD (MIKS, NIPH)
Scientist Kristine B. Gützkow, PhD (MIKS, NIPH)

NTNU
Norwegian University of Science and Technology

Norwegian Institute of Public Health

ACKNOWLEDGEMENTS

The work presented in this thesis was carried out at the Department of Chemicals and Radiation (MIKS), Division of Environmental Medicine, Norwegian Institute of Public Health (NIPH) during the time period from August 2010 to May 2012 for the MSc in Environmental Toxicology and Chemistry at the Norwegian University of Science and Technology (NTNU). My supervisors at MIKS, NIPH have been Scientist Ann-Karin H. Olsen, PhD, and Scientist Kristine B. Gützkow, PhD. Associate Professor Åse Krøkje, PhD, at the Department of Biology, Faculty of Natural Sciences and Technology, NTNU, has served as my internal supervisor at the University.

I would like to thank a number of people who have been particularly important to me during my years as an NTNU student:

First and foremost, I want to thank my great supervisor duo at MIKS; Anka and Kristine. You are simply the best! I would also like to thank you, Gunnar Brunborg (department director), for asking me to write my master's thesis at MIKS. You are a repository of knowledge and creative solutions, and I have learned so much since I started working here as a summer student in 2009! Furthermore, I want to give my thanks to the rest of the very supportive "MIKS'ers", and especially my fellow students Hanne and Kirsti; thank you for all our laughs! In addition, I am particularly grateful to you, Anne, for taking time to help me with logistics in the lab, and more generally for always making me look at the bright side of life during late evenings at MIKS. Moreover, I want to express my gratitude to you, Sissel, you have been such a thoughtful landlady during my stays in Oslo.

Thanks to my fellow students and good friends at Gløshaugen, especially the fabulous Byssus B's; thank you for a GREAT time in Trondheim! It was a blast! A special greeting goes to the other two of The Toxic Three; these last two years wouldn't be the same without you! Last, but not least, my dear family deserves my gratitude for their unconditional love and support, and for always answering my phone calls, regardless of the time of day (or night…).

Oslo, 15th May 2012

Solveig Margrethe Bergseng Lakså

ABSTRACT

DNA lesions are introduced in all living organisms every day, both via endogenous processes and by exposure to an array of DNA damaging agents. DNA lesions require repair for the sustenance of life. Base excision repair (BER) and nucleotide excision repair (NER) are DNA repair pathways involved in removal of oxidative DNA lesions and helix-distorting DNA lesions, respectively. Several studies suggest interactions or crosstalk between these pathways, involving overlapping activities for removal of the same types of DNA lesions but also interference between repair pathways.

Non-repaired DNA lesions are regarded as an important risk factor in the pathogenesis of certain conditions and diseases. It is important to gain insight in the interplay between DNA damaging agents, DNA lesions and their DNA repair pathways, since this may be related to the overall sensitivity of cells to combined exposure to endogenous or exogenous agents.

In the present study, we aimed at studying combined exposures to environmental genotoxicants at low doses, and potential interactions between DNA repair pathways. The two genotoxicants lead to DNA lesions that are processed via two different DNA repair pathways. We studied the impact of low levels of oxidative stress on the repair of low levels of helix-distorting DNA lesions; and – *vice versa* - the impact of low levels of helix-distorting DNA lesions, on the repair of low levels of oxidative DNA lesions. We induced the different types of lesions in cells of different genetic background, to study whether a lack of repair of oxidative DNA lesions could also affect the repair of helix-distorting lesions. For this purpose, we utilised wild type mouse embryonic fibroblasts ($Ogg1^{+/+}$ MEFs), and a MEF cell line deficient in the repair protein 8-oxoguanine DNA glycosylase (Ogg1) ($Ogg1^{-/-}$ MEFs). The *Ogg1* gene is involved in the removal of certain oxidized DNA lesions via BER. $Ogg1^{+/+}$ MEFs exposed to a DNA helix-distorting agent did not show perturbed repair of induced oxidative DNA lesions, suggesting that low levels of NER-sensitive DNA damage do not influence BER. Furthermore, the repair of helix-distorting DNA lesions in wild type MEFs ($Ogg1^{+/+}$) or $Ogg1^{-/-}$ MEFs was not perturbed by a (single) low level exposure to oxidative stress, suggesting that reactive oxygen species (ROS) or BER-sensitive DNA damage do not influence the repair of low levels of helix-distorting DNA lesions. However, $Ogg1^{+/+}$ MEFs showed more efficient repair of helix-distorting DNA lesions compared to $Ogg1^{-/-}$ MEFs, regardless of the level of oxidative lesions present in the DNA. This finding suggests that the

BER-related repair protein Ogg1 may play a role also in the repair of NER-sensitive helix-distorting DNA lesions.

In conclusion, low levels of oxidative stress or helix-distorting DNA lesions did not seem to perturb cellular repair of low levels of helix-distorting DNA lesions or oxidized DNA lesions, respectively, in wild type or Ogg1-deficient MEFs. A crosstalk between Ogg1 and repair of helix-distorting DNA lesions was however observed, suggesting an interplay between BER and NER with respect to the repair of NER-sensitive DNA damage.

SAMMENDRAG

Levende organismer er kontinuerlig utsatt for angrep mot DNA, både via endogene prosesser og ved eksponering for en rekke gentoksiske agens via miljøet. Slike angrep kan forårsake DNA-skader som må repareres for at organismen skal kunne opprettholde sine livsfunksjoner. To av systemene som er involvert i reparasjonen av slike skader er baseeksisjonsreparasjon (BER) og nukleotideksisjonsreparasjon (NER), som reparerer henholdsvis oksidative DNA-lesjoner og heliks-forstyrrende DNA-lesjoner. Flere studier har antydet interaksjoner mellom disse reparasjonssystemene, som f.eks. ved at de overlapper hverandre og reparerer samme type DNA-skade, eller ved at forsinkelse av reparasjonen kan oppstå. Ureparerte skader på DNA er en risikofaktor i utviklingen av visse sykdommer og lidelser.

Det er viktig å øke kunnskapen om samspillet mellom gentoksiske agens, DNA-skader og DNA-reparasjonssystemer, siden slike mekanismer kan ha betydning for cellers totale følsomhet overfor kombinert eksponering for endogene eller eksogene stoffer.

Hensikten med denne studien var å undersøke samspillet mellom lave nivåer av oksidativt stress og reparasjon av lave nivåer av heliksforstyrrende DNA-lesjoner, og motsatt; samspillet mellom lave nivåer av heliksforstyrrende DNA-lesjoner og reparasjon av lave nivåer av oksidert DNA. Dette ble utført ved hjelp av embryonale fibroblaster fra villtypemus (*Ogg1*$^{+/+}$ MEFer) og MEFer fra mus som mangler reparasjonsproteinet 8-oksoguanin DNA glykosylase (Ogg1) (*Ogg1*$^{-/-}$ MEFer). Dette proteinet er involvert i reparasjon av visse oksidative DNA-lesjoner via BER. *Ogg1*$^{+/+}$ MEFer eksponert for DNA-heliksforstyrrende agens viste ingen forsinket reparasjon av oksidative DNA-lesjoner i vårt testsystem, noe som tyder på at lave nivåer av NER-sensitive DNA-skader ikke påvirker BER. Videre ble det vist at reparasjonen av heliksforstyrrende DNA-lesjoner ikke ble forsinket etter en enkelt eksponering for oksidativt stress, verken i villtype-MEFer (*Ogg1*$^{+/+}$) eller i *Ogg1*$^{-/-}$ MEFer. Dette tyder på at verken frie radikaler eller BER-sensitive DNA-skader påvirker reparasjon av lave nivåer av heliksforstyrrende DNA-skader. Det ble imidlertid påvist mer effektiv reparasjon av heliksforstyrrende DNA-lesjoner i *Ogg1*$^{+/+}$ MEFer sammenlignet med *Ogg1*$^{-/-}$ MEFer, uavhengig av mengden oksidative lesjoner til stede i DNA. Dette funnet kan tyde på at proteinet Ogg1, som vanligvis er assosiert med BER, også har en rolle i reparasjonen av NER-sensitive heliksforstyrrende DNA-lesjoner.

Kort oppsummert; lave nivåer av oksidativt stress eller heliksforstyrrende DNA-lesjoner forsinket ikke reparasjonen av henholdsvis heliksforstyrrende DNA-lesjoner eller oksidative DNA-lesjoner, verken i villtype- eller Ogg1-fattige MEFer. Det ble imidlertid observert en sammenheng mellom Ogg1 og reparasjon av heliks-forvridende DNA-lesjoner. Denne sammenhengen tyder på et samspill mellom BER og NER med hensyn til reparasjon av NER-sensitive DNA-skader.

ABBREVIATIONS

6-4PP	6-4 photoproduct
8-oxodG	8-oxo-7,8-dihydro-2'-deoxyguanosine
8-oxo-dGTP	8-oxo-2'-deoxyguanosine-5'-triphosphate
8-oxoG	8-oxo-7,8-dihydroguanine
ANOVA	Analysis of variance
AP lyase	Apurinic/apyrimidinic lyase
AP site	Abasic (apurinic/apyrimidinic) site
B[a]P	Benzo[a]pyrene
BER	Base excision repair
BPDE	Benzo[a]pyrene-7,8-dihydrodiol-9,10-epoxide
BSA	Bovine serum albumin
CPD	Cyclobutane pyrimidine dimer
CSA	Cockayne syndrome factor A
CSB	Cockayne syndrome factor B
dH_2O	Distilled water
DMEM	Dulbecco's Modified Eagle's Medium
DMSO	Dimethyl sulfoxide
DNA	Deoxyribonucleic acid
DSB	Double strand break

E. coli	*Escherichia coli*
EDTA	Ethylenediaminetetraacetic acid
ERCC1	Excision repair cross complementing group 1 protein
ESCODD	European Standards Committee on Oxidative DNA Damage
FapyG	2,6-diamino-4-hydroxy-5-formamidopyrimidine
FCS	Foetal calf serum
FEN1	Flap endonuclease
Fpg	Formamidopyrimidine DNA glycosylase
GGR	Global genomic repair
GPx	Glutathione peroxidase
GSH	Glutathione
HAP1	Human AP-endonuclease 1
hHR23B	Human homologue of yeast RAD23B
HPBL	Human peripheral blood lymphocytes
Lig1	DNA ligase 1
LigIII	DNA ligase III
LPR	Long-patch repair
MEF	Mouse embryonic fibroblasts
MPO	Myeloperoxidase
MutM	Formamidopyrimidine DNA glycosylase

MutT	8-oxodGTPase
MutY	Adenine DNA glycosylase
Myh	MutY homologue
NER	Nucleotide excision repair
Nth1	Thymine glycol DNA glycosylase 1
Ogg1	8-oxoguanine DNA glycosylase
P/S	Penicillin/streptomycin
PAH	Polycyclic aromatic hydrocarbon
PBS	Dulbecco's phosphate buffered saline
PCNA	Proliferating cell nuclear antigen
Polβ	DNA polymerase β
Polδ/ε	DNA polymerase delta/epsilon
RFC	Replication factor C
RNA Pol II	RNA polymerase II
Ro 12-9786	Ethyl-7-oxo-7h-thieno[2,3-A]-quinolizine-8-carboxylate
ROS	Reactive oxygen species
RPA	Replication protein A
SD	Standard deviation
SOD	Superoxide dismutase
SPR	Short-patch repair
SSB	Single strand break
T4endoV	T4 endonuclease V

TCR	Transcription-coupled repair
TFIIH	General transcription factor IIH
UV	Ultraviolet radiation
UVA-C	Ultraviolet radiation, subtype A-C
XPA-G	Xeroderma pigmentosum, complementation group A-G
XPC-hHR23B	Xeroderma pigmentosum C-human homologue of yeast RAD23B
XRCC1	X-ray cross complementing protein 1

Note: The names of proteins are denoted as indicated; humans, e.g. OGG1; rodents, e.g. Ogg1; bacteria, e.g. Fpg. The same rules apply for human and rodent genes in *italic*, whereas *E. coli* genes have a first letter in lower-case (e.g. *fpg*).

TABLE OF CONTENTS

ACKNOWLEDGEMENTS I

ABSTRACT II

SAMMENDRAG IV

ABBREVIATIONS VI

1 INTRODUCTION 1

1.1 General background 1

1.2 Aims 2

1.3 DNA damage 2

1.3.1 Oxidative DNA lesions 2

1.3.2 Helix-distorting DNA lesions 5

1.4 DNA repair 6

1.4.1 Base excision repair (BER) 7

1.4.2 Nucleotide Excision Repair (NER) 9

1.5 Technical issues 11

1.5.1 Mouse embryonic fibroblasts (MEFs) 11

1.5.2 The alkaline single cell gel electrophoresis (comet) assay 12

2 MATERIALS AND METHODS 15

2.1 Cell cultures 15

2.1.1 Culturing conditions 15

2.1.2 Passaging 15

2.1.3 Cell counting 16

2.1.4 Freezing and thawing of cells 16
2.1.5 *Mycoplasma* testing 17
2.2 Induction of DNA damage 17
2.2.1 Experimental design 17
2.2.2 Induction of oxidative DNA lesions 19
2.2.3 Induction of helix-distorting DNA lesions 19
2.3 DNA repair analyses 20
2.4 Cell harvest and isolation 21
2.4.1 Isolation of human peripheral blood lymphocytes (HPBL) from whole blood 21
2.4.2 Harvest of MEFs 21
2.5 Cytotoxicity assessment 22
2.6 The alkaline single cell gel electrophoresis (comet) assay 22
2.6.1 Microscopic analysis of comets (scoring of comets) 25
2.7 Statistical methods 25
3 RESULTS 29
3.1 Establishment of parameters 29
3.1.1 Parameters for oxidative DNA lesions 30
3.1.2 Parameters for helix-distorting DNA lesions 32
3.2 Cell viability 35
3.2.1 Cytotoxicity 35
3.2.2 *Mycoplasma* 36
3.3 Role of low level oxidative stress on repair of helix-distorting DNA lesions 36
3.4 Role of Ogg1 on the repair of helix-distorting DNA lesions 39

3.5 Role of helix-distorting DNA lesions on repair of oxidative DNA lesions 40

4 DISCUSSION 43

4.1 Technical considerations 43

4.2 Effect of oxidative stress on NER 44

4.3 Role of Ogg1 in repair of helix-distorting DNA lesions 47

4.4 Effect of helix-distorting DNA lesions on BER 47

4.5 Conclusions 48

REFERENCES 49

APPENDIX A 53

APPENDIX B 59

APPENDIX C 63

1 INTRODUCTION

1.1 General background

A cell is constantly subjected to attack from environmental and endogenous agents that may cause damage to a variety of molecular targets, including deoxyribonucleic acid (DNA). If these DNA lesions are not removed prior to replication, they can become self-perpetuating mutations that contribute to ageing and degenerative diseases such as cancer (Ames, 1989; Cooke *et al.*, 2003; Floyd, 1990).

A number of DNA repair processes are responsible for removing the variety of DNA lesions caused by genotoxic agents. One of these processes is the nucleotide excision repair (NER) pathway, which is involved in the removal of helix-distorting DNA lesions caused by exposure to e.g. ultraviolet (UV) radiation or chemical carcinogens like polycyclic aromatic hydrocarbons (PAHs). Another pathway is base excision repair (BER), which is responsible for removal of small, non-helix-distorting base lesions resulting from e.g. oxidative stress (Houtgraaf *et al.*, 2006).

Several studies suggest interactions or crosstalk between these pathways, involving overlapping activities for removal of the same types of DNA lesions but also inhibition of repair. A previous study on mice conducted in our lab by Olsen and co-workers indicates such a relationship between BER and NER; hepatocytes of mice deficient of the BER-related repair protein 8-oxoguanine DNA glycosylase (Ogg1) showed a delayed removal of lesions induced by the PAH benzo[a]pyrene (B[a]P) (Olsen, A. K., pers. comm., April 2012). Two recent studies by Langie and co-workers indicate a relationship between oxidative stress and reduced NER capacity, *in vitro* as well as *in vivo* (Langie *et al.*, 2007; Langie *et al.*, 2010).

Impairment of DNA-repair is an important risk factor in the pathogenesis of certain diseases. Therefore, it is important to gain insight in the interplay between DNA damaging agents, DNA lesions and their DNA repair pathways.

1.2 Aims

The overall purpose of this project was to address the following question:

- Can a cell deal with different types of DNA lesions when occurring in its DNA at the same time, and is this important for the cell's overall sensitivity to combinations of environmental and endogenous agents?

In a defined *in vitro* system, our specific aims were:

i) Investigating whether oxidative DNA lesions perturbs the repair of helix-distorting DNA lesions.

ii) Investigating whether helix-distorting DNA lesions perturb the repair of oxidative DNA lesions.

iii) Studying the specific role of the DNA repair protein Ogg1 on the repair of helix-distorting DNA lesions.

1.3 DNA damage

DNA is a complex molecule of limited chemical stability (Watson *et al.*, 2008). It is constantly subject to spontaneous damage by hydrolysis, oxidation, and nonenzymatic methylation, as well as attack by environmental and endogenous agents. Environmental agents include genotoxic chemicals, UV radiation, and ionizing radiation, whereas endogenous threats to the DNA include by-products from cellular metabolism such as reactive oxygen species (ROS) and products of lipid peroxidation (Houtgraaf *et al.*, 2006).

There are several different types of DNA lesions occurring as a result of this constant stress, including altered DNA bases and abasic (apurinic/apyrimidinic) sites (AP sites), single and double strand breaks (SSBs and DSBs, respectively) and helix-distorting lesions such as inter- and intrastrand crosslinks and bulky chemical adducts (Watson *et al.*, 2008).

In this thesis, we will study oxidized DNA bases and helix-distorting lesions and see whether (or how) these two types of lesions in combination may influence the repair of each other.

1.3.1 Oxidative DNA lesions

Oxidative damage to the DNA and other cellular macromolecules is formed as a consequence of attack by ROS, which include hydroxyl radicals ($^{\bullet}OH$), oxygen radicals ($O_2^{\bullet-}$), singlet

oxygen ($^1O_2$), and hydrogen peroxide (H_2O_2) (De Bont and van Larebeke, 2004). The most common source of ROS is from normal cellular metabolism, which accounts for the background level of oxidative DNA lesions that is constantly present in normal cells. In addition, phagocytic cells release ROS during inflammation in order to kill infected cells (Cooke *et al.*, 2003; Evans *et al.*, 2004). ROS may also be formed after exposure to extracellular sources, such as exogenous chemicals (Cooke *et al.*, 2003; Evans *et al.*, 2004), ionizing radiation or UV radiation, subtype A (UVA) (Sinha and Häder, 2002).

As a consequence of the constant exposure to ROS, cells have developed a number of defences to protect DNA against oxidative stress. These defences include low molecular weight compounds such as vitamin C and vitamin E, and more complex enzymes, such as superoxide dismutase (SOD), catalase and glutathione peroxidase (GPx) (Evans *et al.*, 2004).

In spite of antioxidant defences, ROS can induce strand breaks, AP sites and oxidative base lesions. A large number of oxidative base lesions are known, and all four DNA bases can be oxidized. However, guanine is the most prone to oxidation because of its low oxygen potential. One of the most frequently occurring oxidative guanine lesions is 8-oxo-7,8-dihydroguanine (8-oxoG) (Figure 1.1), which is highly mutagenic because of its capability to base-pair both with adenine and cytosine. Base-pairing of 8-oxoG with adenine during replication causes a guanine:cytosine to thymine:adenine transversion, which is one of the most common mutations associated with human cancers (Cooke *et al.*, 2003; Watson *et al.*, 2008). Although 8-oxoG and its deoxyribonucleoside (8-oxodG) are commonly used markers of oxidative DNA lesions, there have been controversies regarding measurement of background levels of 8-oxoG in normal human cells; the background levels are complicated to estimate, as certain methods have been shown to generate additional 8-oxoG in the DNA. However, the European Standards Committee on Oxidative DNA Damage (ESCODD) has estimated the background level of 8-oxoG in normal human cells to be between 0.3 and 4 residues per 10^6 guanines (Collins *et al.*, 2004).

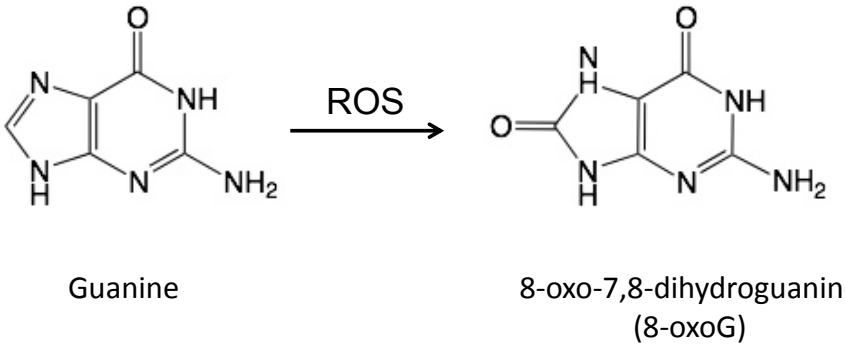

Figure 1.1: ROS-mediated conversion of guanine to 8-oxo-7,8-dihydroguanine (8-oxoG).

Furthermore, when ROS production is greater than the cellular antioxidant capacity, ROS may cause oxidative damage to lipids, proteins, carbohydrates, as well as nucleic acids, thereby compromising their normal functions (Figure 1.2) (Ferguson, 2010). Thus, ROS may directly or indirectly inhibit repair proteins and thus impair DNA repair pathways as suggested in several studies (Güngör *et al.*, 2007; Güngör *et al.*, 2010a; Güngör *et al.*, 2010b; Langie *et al.*, 2007; Langie *et al.*, 2010).

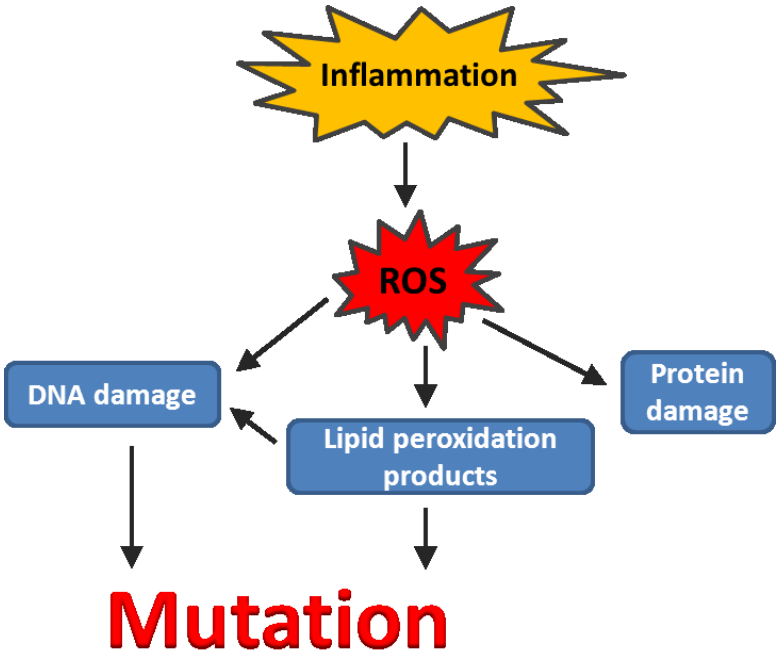

Figure 1.2: A schematic presentation of the relationship between inflammation and ROS-production, DNA damage induction and mutagenesis. Modified from Ferguson (Ferguson, 2010).

1.3.2 Helix-distorting DNA lesions

Distortion of the DNA double helix is known to be caused by sources such as UV radiation and a vast variety of chemicals.

Helix-distorting chemicals include exogenous agents or unfortunate products from their metabolic activation. They often possess electrophilic properties enabling them to bind double-stranded DNA. When such chemicals bind to DNA, bulky DNA adducts are formed (Gillet and Schärer, 2005). An example of such bulky adduct formation takes place after exposure to the environmental pollutant B[a]P. After metabolic activation, the B[a]P metabolite benzo[a]pyrene-7,8-dihydrodiol-9,10-epoxide (BPDE) binds to DNA, forming BPDE-DNA adducts. These adducts are strongly associated with mutations and subsequent tumours (Klaassen, 2001).

Ultraviolet radiation induces another type of helix-distorting DNA lesions, and different UV-induced lesions are formed with different wavelengths of UV. The electromagnetic spectrum of UV is often subdivided dependent on the wavelength; subtype A (UVA, 400 – 315 nm), B (UVB, 315 – 280 nm), or C (UVC, 280 – 100 nm) (Sinha and Häder, 2002).

Wavelengths within the UVA spectrum are not absorbed by DNA; hence they are less efficient in inducing DNA damage. However, they are still capable of causing DNA damage via indirect photosensitizing reactions, such as the generation of $^1O_2$ through type II photosensitisation reactions, or via secondary photoreactions of existing DNA photoproducts (Sinha and Häder, 2002).

During UVB and UVC irradiation, photo excited thymine and/or cytosine in DNA react with adjacent pyrimidine bases, leading to formation of photoproducts (Figure 1.3) (Sinha and Häder, 2002). Two major classes of photoproducts are produced: The cyclobutane pyrimidine dimers (CPDs) and the 6-4 photoproducts (6-4PPs) (Sinha and Häder, 2002; Taylor *et al.*, 1990). Moreover, upon exposure to wavelengths above 280 nm, 6-4PPs are further converted (Taylor *et al.*, 1990), such as the photo isomerisation into Dewar isomers (Mitchell and Nairn, 1989).

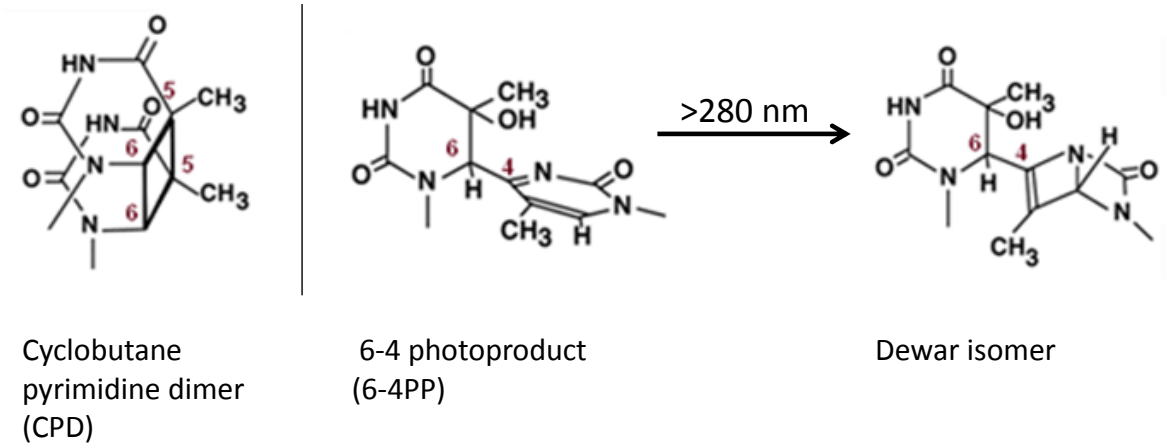

Figure 1.3: UV-induced DNA lesions (modified from http://www.cosmobio.co.jp/export_e/products/antibodies/products_cac_20080404.asp?entry_id=3597).

Helix-distorting lesions caused by UV can interfere with DNA transcription and replication if they are not repaired. This interference can lead to misreading of the genetic code, which can eventually cause mutations and even cell death.

1.4 DNA repair

Damage to DNA can have consequences such as inhibition of replication and/or transcription, or permanent alteration of the DNA. Ultimately these scenarios can cause mutations, cancer or cell death. Therefore, cells have evolved several defence mechanisms to combat induction and persistence of DNA damage. Firstly, formation of DNA damage can be prevented by agents such as antioxidants and detoxifying enzymes. Secondly, a cell with damaged DNA can be eliminated by apoptosis or spontaneous death. Thirdly, damaged DNA can be identified and removed by various DNA repair pathways, including direct reversal, mismatch repair, homologous recombination, non-homologous end joining and excision repair. The repair strategy employed in DNA damage removal is dependent on lesion characteristics (Watson *et al.*, 2008).

In this thesis, we focus on the excision repair pathways, which are responsible for removal of damaged nucleotides followed by a replacement with undamaged nucleotides complementary to the undamaged DNA strand. Two different excision repair pathways exist; base excision repair (BER) (Figure 1.4) and nucleotide excision repair (NER) (Figure 1.5).

1.4.1 Base excision repair (BER)

Base excision repair (Figure 1.4) is the major pathway for removal of small, non-helix-distorting base lesions in the size range of one to ten bases. These lesions can be caused by oxidation (such as 8-oxoG), alkylation, hydrolysis, or deamination.

The repair pathway is initiated by a lesion-specific glycosylase. This enzyme recognises and removes the damaged base by hydrolytic cleavage of the glycosylic bond between the base and deoxyribose. The resulting AP site is removed by an apurinic/apyrimidinic lyase (AP lyase), creating a nick in the DNA backbone. Dependent on the number of bases incised, two sub-pathways are responsible for further completion of BER (Krokan *et al.*, 2000).

In short-patch repair (SPR), which is the predominant BER pathway, a single nucleotide is incorporated, whereas in long-patch repair (LPR), two to ten nucleotides are incorporated into DNA. Although the two pathways make use of different enzymes and enzyme complexes, they have similar functions; both make use of a DNA polymerase to incorporate undamaged nucleotides, followed by sealing of the remaining nick by a DNA ligase (Krokan *et al.*, 2000).

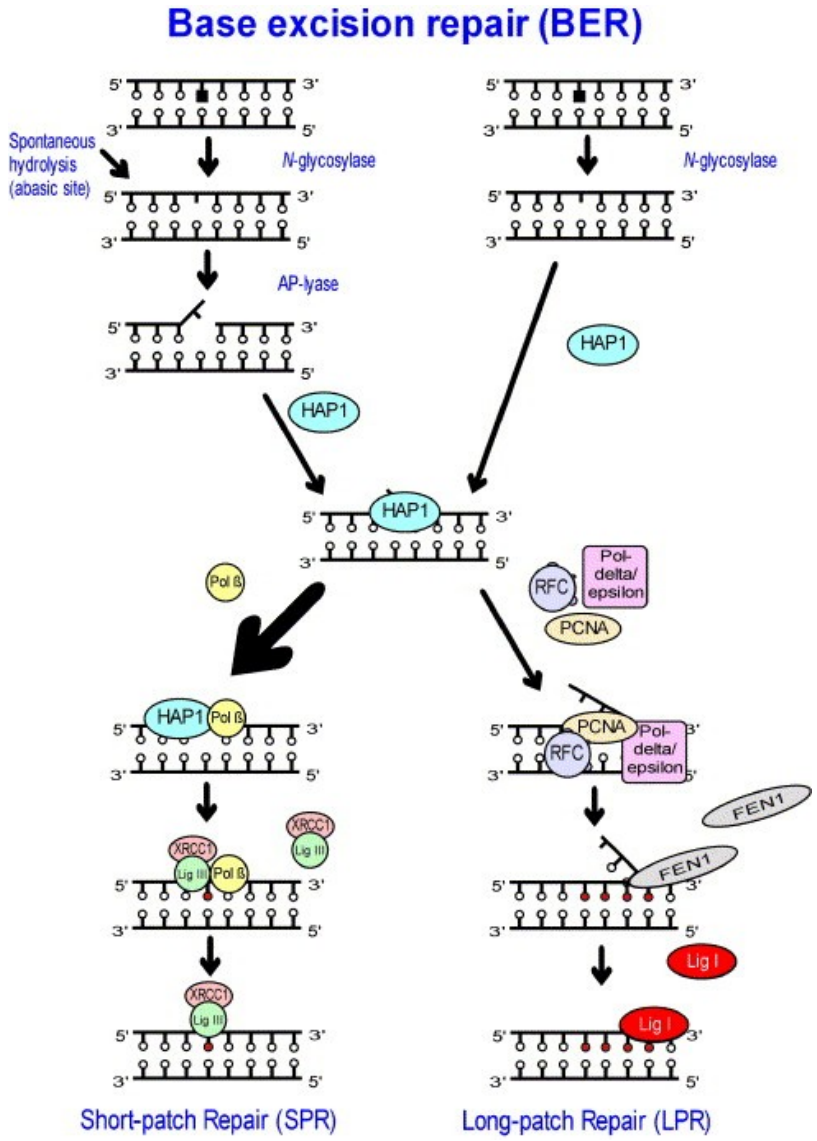

Figure 1.4: An outline of the BER pathway. See text for description of the pathway. Abbreviations in chronological order: HAP1, human AP-endonuclease 1; Polβ, DNA polymerase β; XRCC1, X-ray cross complementing protein 1; LigIII, DNA ligase III; PCNA, proliferating cell nuclear antigen; RFC, replication factor C; Polδ/ε, DNA polymerase delta/epsilon; FEN1, Flap endonuclease; Lig1, DNA ligase 1. The figure is modified by Olsen *et al.* (Olsen *et al.*, 2005) from Ide and Kotera (Ide and Kotera, 2004).

1.4.1.1 DNA glycosylases acting upon 8-oxoG lesions and CPDs

Several DNA glycosylases have been identified in both procaryotes and eucaryotes. There are two subgroups of DNA glycosylases; mono-functional glycosylases, which only removes the damaged base, and bi-functional glycosylases, which also function as AP lyases.

Here, the attention will be pointed at glycosylases acting upon 8-oxoG lesions and CPDs.

Escherichia coli (*E. coli*) bacteria have developed three important enzymes for removal of 8-oxoG lesions; 8-oxodGTPase (MutT), adenine DNA glycosylase (MutY), and formamidopyrimidine DNA glycosylase (Fpg/MutM). MutT eliminates the oxidized nucleotide 8-oxo-2'-deoxyguanosine-5'-triphosphate (8-oxodGTP), MutY excises the adenine of a guanine:adenine mispair, whereas Fpg removes 8-oxoG paired with cytosine (Krokan *et al.*, 1997).

In mammalian cells, the two glycosylases thymine glycol DNA glycosylase 1 (Nth1) and MutY homologue (Myh) are orthologs for MutT and MutY, respectively. Ogg1 is a functional homologue for Fpg and it removes 8-oxoG and 2,6-diamino-4-hydroxy-5-formamidopyrimidine (FapyG) lesions, which results in the formation of AP sites (Krokan *et al.*, 1997).

After infecting *E. coli* with the bacteriophage T4 (a bacterium-infecting virus) these bacteria starts producing an enzyme denoted as T4 endonuclease V (T4endoV) (Yasuda and Sekiguchi, 1970). This enzyme is a bi-functional glycosylase, and recognizes and removes CPDs produced by UV irradiation (Sinha and Häder, 2002). Since production and purification of T4endoV is relatively easy to perform (Friedberg *et al.*, 1980), the enzyme is frequently used to study induction of UV-induced lesions.

In mammals, there is no glycosylase homologue for T4endoV. The explanation for this is that in mammals, the NER pathway is responsible for removal of UV-induced DNA lesions such as CPDs (Sinha and Häder, 2002).

1.4.2 Nucleotide Excision Repair (NER)

Nucleotide excision repair (Figure 1.5) is the most important pathway for recognition and removal of helix-distorting lesions, such as CPDs and 6-4PPs (Gillet and Schärer, 2005). Products of around 30 genes are employed by NER, and defects in one or more of these repair proteins are associated with elevated risk of cancer (Cleaver, 1989; Sinha and Häder, 2002).

There are two modes of activation of the NER pathway; global genomic repair (GGR) and transcription-coupled repair (TCR).

The GGR pathway detects lesions in non-transcribed parts of the entire genome, including non-transcribed strands of transcribed genes. Initiation of GGR takes place by binding of an

enzyme complex (xeroderma pigmentosum C-human homologue of yeast RAD23B (XPC-hHR23B)) to a damage-containing oligonucleotide (Gillet and Schärer, 2005).

The TCR pathway, on the other hand, is responsible for recognising DNA damage that is blocking RNA polymerase in transcribed strands of active genes. This is carried out by displacement of the lesion-blocked polymerase, making the DNA lesion accessible for repair. The initiation of TCR requires at least two TCR-specific factors; the cockayne syndrome factors A and B (CSA and CSB, respectively). This is followed by unwinding of about 30 base pairs surrounding the DNA by means of a lesion multi-protein complex. This complex includes the two helicases xeroderma pigmentosum complementation group B and D (XPB and XPD, respectively).

The subsequent steps of GGR and TCR are believed to be identical (Missura *et al.*, 2001).

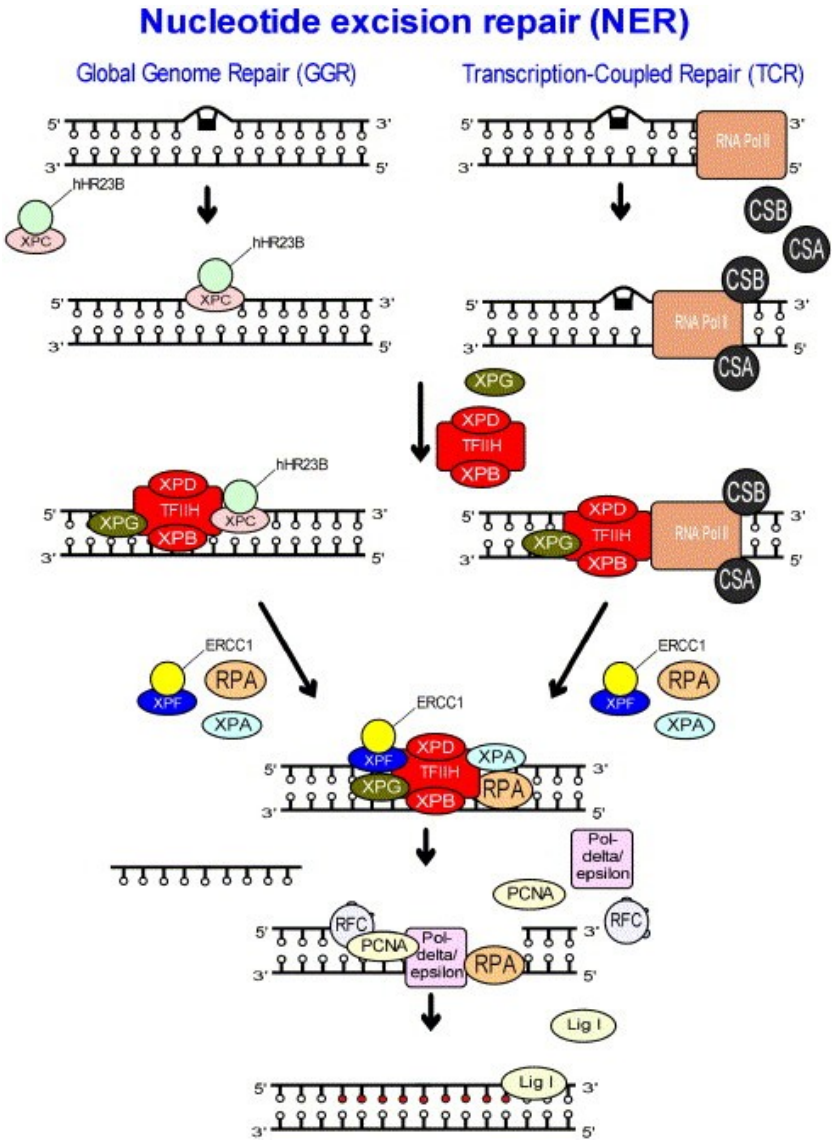

Figure 1.5: An outline of the NER pathway. See text for description of the pathway. Abbreviations in chronological order: XPA–G, xeroderma pigmentosum complementation group A–G; hHR23B, human homologue of yeast RAD23B; RNA Pol II, RNA polymerase II; CSA and CSB, Cockayne syndrome factors A and B; TFIIH, general transcription factor IIH; ERCC1, excision repair cross complementing group 1 protein; RPA, replication protein A; PCNA, proliferating cell nuclear antigen; RFC, replication factor C; Polδ/ε, DNA polymerase delta/epsilon; Lig1, DNA ligase 1. Figure from Olsen *et al.* (Olsen *et al.*, 2005).

1.5 Technical issues

1.5.1 Mouse embryonic fibroblasts (MEFs)

Mouse embryonic fibroblasts (MEFs) are isolated from mid-gestation mouse embryos. Isolation of MEFs is relatively easy to perform, and since these cells can be derived from mice carrying various genetic alterations, MEFs are ideal for studying aspects of functional

genetics (Kamijo *et al.*, 1997; Lowe *et al.*, 1994; Steinman *et al.*, 2004). In this study, we used embryonic fibroblasts from wild type (*Ogg1*$^{+/+}$) and Ogg1 deficient (*Ogg1*$^{-/-}$) mice (*Ogg1*$^{+/+}$ and *Ogg1*$^{-/-}$ MEFs).

1.5.1.1 *Ogg1* knock-out mouse model

For the purpose of learning more about the relevance of the DNA glycosylase Ogg1 in mammals, Klungland *et al.* (Klungland *et al.*, 1999) generated homozygous *Ogg1*$^{-/-}$ null mice. This mouse model was developed by targeted disruption of the *Ogg1* gene in murine embryonic stem cells (from 129SV mice) followed by injection of these cells into blastocysts (from C57BL/6J mice), resulting in heterozygous mice. Furthermore, the mice were interbred, yielding homozygous *Ogg1*$^{-/-}$ mutants, which accumulate abnormal levels of 8-oxoG and Fpg-sensitive sites in their genome (Klungland *et al.*, 1999).

1.5.2 The alkaline single cell gel electrophoresis (comet) assay

The comet assay is a method used for DNA damage measurements and repair assessments, and measures DNA strand breaks in individual cells (Ostling and Johanson, 1984; Singh *et al.*, 1988). Cells exposed to a genotoxic agent are embedded in agarose and moulded onto a plastic support as described in Hansen *et al.* (Hansen *et al.*, 2010). Cells are put in lysis solution to remove non-DNA components such as membranes and organelles, followed by unwinding and electrophoresis of DNA. During electrophoresis, structures resembling comets are formed; relaxed loops will extend from the nucleoid core toward the anode, forming a tail (Figure 1.6). Comets are stained with a fluorescent dye and observed by fluorescence microscopy, and the intensity of the comet tail relative to the head DNA intensity represents the quantity of DNA strand breaks. Furthermore, as described in Olsen *et al.* (Olsen *et al.*, 2003), Hansen *et al.* (Hansen *et al.*, 2010), and Duale *et al.* (Duale *et al.*, 2010), the use of lesion-specific endonuclease-extracts provides the opportunity to reveal specific DNA lesions in the comet assay.

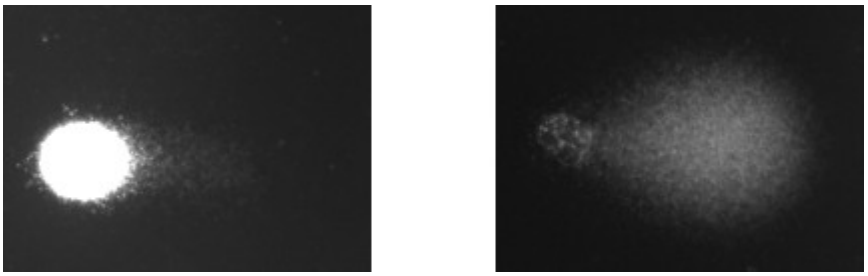

Figure 1.6: Image of comets. Comet DNA stained with a fluorescent dye and observed by fluorescence microscopy. The intensity of the comet tail represents the quantity of DNA strand breaks in a single cell. Undamaged DNA to the left, damaged DNA to the right.

2 MATERIALS AND METHODS

All media and solutions used are described in Appendix B.

2.1 Cell cultures

Mouse embryonic fibroblasts (MEFs) from WT (*Ogg1*$^{+/+}$) mice or genetically modified mice, where the repair gene Ogg1 has been deleted (*Ogg1*$^{-/-}$), were used for all experiments (except for titration of the endonuclease T4endoV-extract, where human peripheral blood lymphocytes (HPBL) were used). The MEF cell cultures were kindly given to us by Professor Lars Eide at the Department of Medical Biochemistry, Oslo University Hospital.

2.1.1 Culturing conditions

The cell cultures were grown in Dulbecco's Modified Eagle's Medium (DMEM) containing foetal calf serum (FCS), L-glutamine and penicillin/streptomycin (P/S) (growth medium) at 37 °C with 5 % CO_2 in air under saturated humidity in cell cultivator.

2.1.2 Passaging

The growth of cells in culture follows a visually recognisable pattern. After seeding, the cells enter a lag period, followed by a phase of exponential growth. With a split ratio of 1:5 (*Ogg1*$^{+/+}$) or 1:10 (*Ogg1*$^{-/-}$), the MEF cultures reached confluence approximately four days after seeding. Since confluent MEFs in culture stop proliferation and initiate differentiation, the cultures required passaging every fourth day.

Procedure:

All steps from b) were performed under sterile conditions under laminar flow using sterile equipment. All the equipment was sprayed with 70 % ethanol before entering the laminar flow bench.

a) Trypsin (0.05 % trypsin, 0.1 mmol/l ethylenediaminetetraacetic acid (EDTA)), phosphate buffered saline (PBS) and growth medium were preheated to 37 °C.

b) The growth medium in the culture flasks was removed and the cells were washed twice with 10 ml PBS (162 cm² flask) to remove the growth medium, as FCS from the growth medium inhibits the trypsin.

c) To detach the adherent cells from the bottom of the culture flask (162 cm^2), 1 ml trypsin was applied to the cells, followed by incubation for approximately 1-2 min at 37 °C in the cell incubator. The cells were released from the flask by tapping the sides and the bottom.

d) The trypsin was inactivated by applying 9 ml of growth medium. The cells were homogenised and separated by pipetting.

e) A 1 ml portion of the cell suspension was transferred to a new cell culture flask (162 cm^2), containing 29 ml of fresh growth medium (1:10 split ratio), and resuspended to homogeneity. Date, cell line, passage number and dilution ratio was noted, and the cells were cultivated at 37 °C in the cell incubator.

f) Cells intended for experiments were plated using a 1:2 ($Ogg1^{+/+}$) or 1:4 ($Ogg1^{-/-}$) split ratio in 2 ml portions in 35 mm cell culture dishes and incubated for 24 h before exposure.

2.1.3 Cell counting

Cell concentration (cells/ml) was calculated by placing 10 µl of cell suspension on to a hemocytometer (Bürker chamber), counting the cells observed in five squares, and multiplying the average number of cells from the squares with 10^4.

2.1.4 Freezing and thawing of cells

Freezing:

a) Growth medium was changed 24 h before freezing.

b) The cells (~80 % confluent) were trypsinated according to procedure described in section 2.1.2 a) – d), followed by adding of 14 ml growth medium.

c) Cells were counted according to procedure described in section 2.1.3, followed by centrifugation at 8 °C and 200 × *g* for 5 min.

d) Cells were placed on ice, supernatant was removed and the pellet was resuspended in 6 ml growth medium containing 10 % dimethyl sulfoxide (DMSO).

e) The cell suspension was transferred to cryotubes (1.8 ml) and kept at 4 °C for 5 min.

f) Cryotubes were placed in the lower row of a freezing unit in a nitrogen tank for 3-4 h, and were then transferred to liquid nitrogen.

Thawing:

a) The cells were defrosted in a preheated water bath at 37 °C for 2-3 min, after which cell line and passage number were noted before spraying the tube with 70 % ethanol.

b) The cells were then transferred into a 15 ml centrifuge tube containing 13 ml preheated growth medium, followed by centrifugation at 8 °C and 200 × *g* for 5 min.

c) Supernatant was removed and the pellet was resuspended in 15 ml medium.

d) The cell suspension was transferred to a 75 cm² cell culture flask and incubated at 37 ºC.

The cells were allowed to grow for three to five days before passaging, as initial growth after defrosting is slow. To make sure the cells were attached to the bottom of the flask, control checks under a microscope were performed every day.

2.1.5 *Mycoplasma* testing

Immunofluorescence test for the detection of *Mycoplasma* species in our cell cultures was conducted according to the protocol enclosed in the RIDA®FLUOR *Mycoplasma* IFA immunofluorescence assay kit from R-Biopharm AG.

2.2 Induction of DNA damage

Several considerations were taken into account with respect to induction of DNA damage. First, two kinds of DNA damage were to be induced; oxidative DNA base damage, by means of exposing the cells to the photosensitiser ethyl 7-oxo-7h-thieno[2,3-A]-quinolizine-8-carboxylate (Ro 12-9786) in the presence of light (Ro 12-9786 plus light), and helix-distorting DNA lesions induced by exposing cells to UVC radiation. The reduction of these levels of DNA damage was to be measured in the comet assay, to assess DNA repair. Secondly, both types of DNA damage were to be present simultaneously in the cells, to understand the impact of one type of DNA damage on the repair of the other. The level of interfering DNA damage should be in the upper part of the dynamic range of the comet assay, to be present during a significant time of the following repair period. Dose-response curves were hence established.

2.2.1 Experimental design

Two separate experiments were designed (Figure 2.1). One of these experiments was designed to help us understand the impact of oxidative DNA lesions on the repair of helix-

distorting DNA lesions. Another purpose of this experiment was to investigate the role of the DNA repair protein Ogg1 on the repair of the mentioned helix-distorting DNA lesions. We denote this experiment "Study 1". Contrary, the other experiment was designed to investigate the impact of helix-distorting DNA lesions on the repair of oxidative DNA lesions. This experiment is denoted "Study 2".

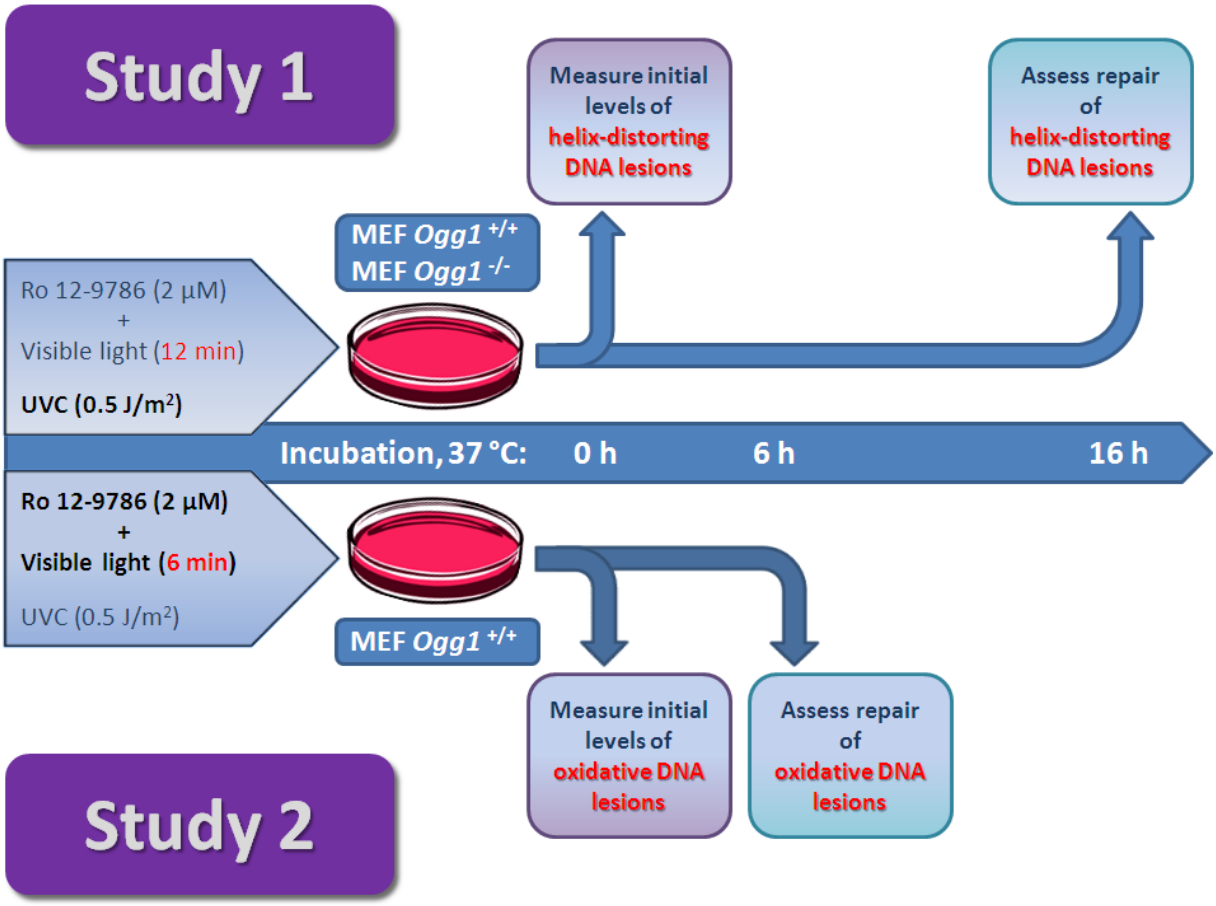

Figure 2.1: Experimental design giving an outline of Study 1 and Study 2.

2.2.1.1 Study 1

The cells (*Ogg1*$^{+/+}$ and *Ogg1*$^{-/-}$ MEFs) were exposed to Ro 12-9786 plus light and UVC. Two biological replicas were included for each treatment; one of which was harvested immediately after exposure, whereas the other one was harvested after 16 h of incubation (37 °C) (Figure 2.1). Three controls were included; an unexposed (negative) control, a control exposed to UVC and light and a control exposed to UVC and Ro 12-9786.

2.2.1.2 Study 2

The cells (*Ogg1*$^{+/+}$ MEFs only) were exposed to Ro 12-9786 plus light and UVC. Two biological replicas were included for each treatment, one of which was harvested immediately after exposure, whereas the other one was harvested after 6 h of incubation (37 °C) (Figure 2.1). Three controls were included; an unexposed (negative) control, a control exposed to Ro 12-9786 alone and a control exposed to Ro 12-9786 plus light.

2.2.2 Induction of oxidative DNA lesions

To induce oxidative DNA lesions, the photosensitiser Ro 12-9786 was used. This compound was originally developed by Roche as an antipsychotic drug, but was discarded during genotoxicity screening due to its photomutagenic activity (Gocke *et al.*, 1998). When irradiated with visible light in presence of oxygen, photosensitisers such as Ro 12-9786 produces high quantities of ROS (Gocke *et al.*, 1998), which in turn induces oxidative purine modifications such as 8-oxoG (Schneider *et al.*, 1990) without introducing high levels of SSBs.

Procedure:

The samples (cells in culture dishes) were kept on a cool metal plate in dim light.

a) Samples were treated with 2 µM Ro 12-9786 by adding 3.3 µl of 1.2 mM Ro 12-9786 stock solution directly into the cell culture dishes (containing cells and 2 ml of growth medium). Ro 12-9786 was mixed into the growth medium by swirling the cell culture dishes.

b) The samples were allowed to rest for 1 min to allow Ro 12-9786 to enter the cells, followed by irradiation of the cells for 6 or 12 min with visible light (halogen light, 500 W) at a 15 cm distance. Lids were removed from the cell culture dishes prior to visible light exposure.

c) The exposure was stopped by removing the medium from the dish and washing three times with PBS (2 ml) followed by adding fresh growth medium (2 ml).

2.2.3 Induction of helix-distorting DNA lesions

During UVC exposure, photoexcited thymine and/or cytosine react with adjacent pyrimidine bases (as seen in Figure 1.3), leading to formation of two major classes of photoproducts detectable by NER: The CPDs and the 6-4PPs (Sinha and Häder, 2002; Taylor *et al.*, 1990). Moreover, upon exposure to wavelengths above 280 nm, 6-4PPs are further converted (Taylor

et al., 1990), such as the photoisomerisation into Dewar isomers (Mitchell and Nairn, 1989). Tungsten-halogen lamps, like the one used to induce oxidative lesions in our experiments, produce a broad spectrum of wavelengths, and can thus lead to such photoisomerisation. The Dewar isomers are alkali-sensitive (Mitchell and Nairn, 1989), and may consequently appear as SSBs in the comet assay, due to the alkaline conditions during lysis, unwinding and electrophoresis. Therefore, the order of exposure of cells exposed to both Ro 12-9786 plus light and UVC is important: To limit the presence of Dewar isomers that would appear in the comet assay as SSBs, the samples should be exposed to Ro 12-9786 plus light before UVC exposure.

Procedure:

The samples were kept on a cold metal plate in dim light.

a) The UVC lamp was preheated for 15 min prior to exposure to ensure continuous irradiation.

b) Cell samples in 35 mm cell culture dishes with growth medium (2 ml) were exposed to UVC. Lids were removed prior to irradiation.

c) Some samples were incubated to allow repair, whereas others were used to assess initial DNA damage levels in the comet assay.

2.3 DNA repair analyses

The cells incubated for DNA repair were harvested 16 h (Study 1) or 6 h (Study 2) after exposure, and the reduction of DNA damage levels was to be measured in the comet assay, to assess DNA repair. The repair capacity was calculated by subtracting the damage level in repaired cells from the damage level in unrepaired cells, yielding a difference representing the total amount of DNA repaired after 16 h of incubation. Furthermore, this difference was converted into a percentage relative to the initial damage level.

2.4 Cell harvest and isolation

2.4.1 Isolation of human peripheral blood lymphocytes (HPBL) from whole blood

Blood samples were obtained by venipuncture from healthy volunteers. Lymphocytes were isolated by Ficoll-Hypaque density gradient as follows:

a) Whole blood was diluted 1:1 with PBS and transferred to a ready-made lymphoprep^{TM} tube. The tube was centrifuged for 20 min and 500 × *g* at room temperature.

b) The layer of mononuclear cells was transferred to a centrifuge tube, washed with PBS and centrifuged at 800 × *g* at room temperature for 5 min.

c) The pellet was resuspended in PBS, cells were counted and diluted in PBS to the desired cell concentration, preferably 1×10^6 cells/ml.

2.4.2 Harvest of MEFs

PBS, growth medium and samples were kept on ice.

a) The growth medium was removed from the cell culture dishes, followed by washing twice with PBS (2 ml).

b) Two drops of trypsin was applied to each dish, followed by incubation for approximately 1-2 min at 37 °C. The cells were released from the surface by tapping the sides of the dish.

c) Trypsination was stopped by applying 1.5 ml of growth medium to each dish.

d) Cells were transferred to 1.5 ml Eppendorf tubes and centrifuged at 300 × *g* at 4 °C for 6 min.

e) The supernatant was removed and the pellet was resuspended in 400-600 µl of growth medium to obtain a concentration of approximately 1×10^6 cells/ml, which is suitable for the comet assay.

2.5 Cytotoxicity assessment

To make sure that the doses given during Ro 12-9786 plus light and UVC exposure did not exert cytotoxic effects, cytotoxicity assessment was conducted by means of the trypan blue exclusion test.

When stained with trypan blue, live cells with intact membranes will exclude the dye, whereas dead or damaged cells will absorb the dye and appear blue under the microscope. Thus, the number of blue cells gives an indication of cytotoxicity.

Procedure:

a) A 10 µl portion of cell suspension was stained with 10 µl trypan blue. The cells were allowed to rest for 5 min, to allow the trypan blue dye to enter the dead and damaged cells.

b) The dyed cell suspension (10 µl) was placed on to a hemocytometer (Bürker chamber), and the number of blue stained cells as well as the number of intact cells was noted.

c) The viability percentage was calculated by dividing the number of living cells by the number of total cells and multiplying by 100.

2.6 The alkaline single cell gel electrophoresis (comet) assay

The comet assay is a simple and sensitive method for measuring DNA strand breaks in individual eukaryotic cells (Ostling and Johanson, 1984; Singh *et al.*, 1988): Cells exposed to a genotoxic agent are embedded in agarose and moulded onto the hydrophilic side of a plastic support such as the GelBond® film, as described by Hansen *et al.* (Hansen *et al.*, 2010). Embedded cells are immediately put in lysis solution to remove membranes, cytoplasm and nucleoplasm and the high salt concentration solubilises most of the histones, consequently the nucleosomes are disrupted. Prior to electrophoresis the embedded cells are put in high alkali solution (pH >13.2) resulting in unwinding of the supercoiled DNA, and loops containing one or more strand breaks will be relaxed. During electrophoresis, structures resembling comets are formed; relaxed loops will extend from the nucleoid core toward the anode, forming a tail. Comets stained with a fluorescent dye are observed by fluorescence microscopy, and the intensity of the comet tail relative to the head DNA intensity represents the quantity of DNA strand breaks.

In addition to DNA strand breaks, the comet assay also detects alkali-labile sites, i.e. lesions capable of being transformed into SSBs under alkaline conditions, such as AP sites. However, strand breaks and alkali-labile sites are not the only kind of damage present in DNA; other types of DNA damage include lesions such as oxidised bases and UV-induced DNA lesions. The use of lesion-specific endonucleases provides the opportunity to reveal specific DNA lesions in the comet assay: The different enzymes recognise a specific kind of damage and convert the damage into strand breaks detectable by the comet assay.

Simultaneously with enzyme incubation, it is recommended to incubate a replicate film in enzyme buffer alone revealing SSBs and alkali-labile sites. The comet score from each sample in the controls can then be subtracted from the comet score obtained in the enzyme treated film, giving a net amount of enzyme-sensitive sites (Collins *et al.*, 2008).

As described by Olsen *et al*. (Olsen *et al.*, 2003), Hansen *et al.* (Hansen *et al.*, 2010) and Duale *et al*. (Duale *et al.*, 2010), respectively, protein-extracts from an over-producing plasmid in *E. coli* expressing the DNA glycosylases Fpg or T4endoV were utilised in our experiments.

Fpg detects oxidised purines such as 8-oxoG, as well as ring-opened purines, or formamidopyrimidines, and AP sites. However, since AP sites are alkali-labile, they are detected as SSBs in the controls and thus not included as enzyme-sensitive sites (Collins *et al.*, 2008).

T4endoV recognises UV-induced CPDs.

The Fpg- and T4endoV-extracts used in our experiments tend to exert unspecific endonuclease activity at high concentrations. Therefore, the enzyme activities had to be titrated against well-known damage levels in order to obtain the optimal enzyme concentration for each experimental set up. In addition, as the comet assay is a sensitive method, it easily saturates the system in cases where nearly all DNA is in the tail (highly damaged DNA). Due to the dynamic range of the comet assay, it was necessary to find the optimal dose for the different genotoxic exposures using Ro 12-9786 and light irradiation, as well as UVC exposure. Dose response curves were conducted, using different concentrations of Fpg- and T4endoV-extracts.

The comet assay procedure:

All steps were performed in dim light.

a) Low melting point agarose (0.75%), lysis solution and electrophoresis buffer was prepared (as described in Appendix B). The agarose was kept at 37 °C, whereas the lysis solution and the electrophoresis buffer were kept at 4 °C.

b) The films were placed on a cold metal plate and the cells were mixed with agarose in a 1:10 dilution. For each sample, cell-agarose gel suspension (5 µl) was moulded onto the films by means of an 8-multichannel pipette.

Each sample was moulded in triplicates onto three separate GelBond® films; two films were prepared for enzyme treatment (Fpg and T4endoV-extract), while one was prepared for enzyme reaction buffer treatment (without enzyme).

c) The films were placed in lysis solution over night at 4 °C. The next day, films were briefly rinsed in distilled water (dH_2O) prior to pre-treatment with enzyme reaction buffer for 10 min followed by another 50 min in a new round of fresh buffer.

d) For enzyme treatment, enzyme reaction buffer containing 0.2 mg/ml bovine serum albumin (BSA) was pre-warmed to 37 °C before adding crude Fpg- or T4endoV-extract to attain the final concentrations of 0.05 µg/ml and 15 µg/ml, respectively. The films were subsequently incubated in enzyme reaction buffer with or without enzyme at 37 °C for 1 h.

e) Unwinding of DNA was performed by placing the films in electrophoresis buffer (pH 13.2) at 4 °C for 5 min and then 35 min in a new round of fresh buffer.

f) The films were placed in fresh electrophoresis buffer, and gel electrophoresis was carried out at 8 °C, 25 V and ~700 mA, for 25 min. The voltage drop across the platform was approximately 0.9 V/cm.

g) The films were neutralised by placing them twice in fresh neutralising buffer for 5 min at room temperature.

h) Films were then rinsed in dH_2O prior to fixation in absolute ethanol for 5 min, followed by 1.5 h fixation in fresh absolute ethanol.

i) The films were allowed to dry before storage in a dark place at room temperature until DNA staining with SYBR® Gold.

j) The comets were stained by placing each film in 40 ml TE-buffer mixed with 40 µl of SYBR® Gold (1000× diluted stock in DMSO). The comets were dyed for 20 min after which they were rinsed in dH_2O and covered with a glass cover slip. Prior to microscopic analysis (scoring of comets), the films were stored moist, dark and cold (8 °C). The films were analysed within three days.

2.6.1 Microscopic analysis of comets (scoring of comets)

Scoring of the comets was conducted using an Olympus BX51 microscope with an Olympus Burner with a Mercury Short-Arc HBO® 100 W/2 lamp and an A312f camera. The camera was linked to a computer with the image analysis software "Comet assay IV".

When illuminated, the fluorescent SYBR® Gold stain bound to the comet DNA emits visible light. This feature makes it possible for the image analysis software to calculate the light intensity of the comet head and tail. The per cent tail DNA intensity relative to the head DNA intensity is used as a measure of damage, as it increases linearly with break frequency (Lovell and Omori, 2008). The comets were selected by the operator, and a total of 100 comets were scored for each group of three technical replicates. As the software is not capable of discriminating regular comets from overlapping comets and artefacts, the latter were deliberately avoided by the operator.

2.7 Statistical methods

Currently, there is no consensus on a standard statistical method for the analysis of comet data (Lovell and Omori, 2008). A reason for this may be the tendency of comet data to have a complex distribution dependent on damage levels: Generally, data from lesser damaged cells tend to skew to the right, whereas data from cells with high damage levels tend to skew to the left compared to a normal distribution. Unfortunately, log-transformation of the data is of little use, as only the right skewed data would be normalised.

Another important consideration in the statistical analysis of comet experiments is the concept of the experimental unit. According to a review by Lovell and Omori (Lovell and Omori, 2008), an experimental unit is defined as “the smallest amount of experimental material that

can be randomly assigned to a treatment". In our experiments, this equals the subculture of differently exposed cells originating from a mutual cell culture.

Significant but artifactual differences between differently exposed subcultures may be obtained if each cell within a cell subculture is treated as the experimental unit. Instead, Lovell and Omori (Lovell and Omori, 2008) recommend including replicate subcultures (biological replicas) in the experiment. This solution provides a valid estimate of subculture variability and a valid, if low power, test of the treatments for that specific subculture. However, this solution would have been logistically impossible to carry out in our experiments, as it would involve a number of subcultures too high to handle without compromising the results. Instead, we aimed at running several identical experiments. However, the first of the experiments had to be discarded due to unacceptably high background DNA damage levels in the exposed samples.

The restricted number of experiments resulted in a low statistical power and thus no statistical significance was obtained, even though an obvious difference was observed. The standard deviation of the two separate experiments in each of the studies (Study 1 and Study 2) gives a better visual presentation regarding the variability between them. However, if the number of experiments in each study were to be increased, we would test the data according to the following argumentation:

Parametric tests rely on assumptions of independence, homogenous variances and normality. Accordingly, the parametric t-test strictly requires the data to be normally distributed. Since comet data tend to deviate from normality, we prefer the non-parametric Mann-Whitney U test to compare the damage levels before and after repair, and the levels of repair in the differently exposed subcultures.

On the other hand, when comparing the repair capacity between the two MEF genotypes, $Ogg1^{+/+}$ and $Ogg1^{-/-}$ (each of the two groups containing three different exposure scenarios), analysis of variance (ANOVA) is preferred. The reason for this is that ANOVA, although being a parametric test, is sufficiently robust to be used with data exhibiting differences in variance (with a factor of 2-5) and with small violations of the normality.

The statistical program used was SigmaPlot version 11.0 for Windows. Results were regarded significantly different from each other at a significance level below 0.05. Otherwise,

Microsoft Office Excel 2010 for Windows was used to prepare figures and to calculate mean and standard deviation of each sample.

3 RESULTS

Two separate series of experiments (Study 1 and 2, Figure 2.1) were carried out. The purpose of the first study (Study 1) was to investigate the impact of oxidative DNA lesions on the repair of helix-distorting DNA lesions. A second purpose of Study 1 was to investigate whether the DNA repair protein Ogg1 is involved in the repair of helix-distorting DNA lesions. The second study (Study 2) was designed in order to investigate the impact of helix-distorting DNA lesions on the repair of oxidative DNA lesions.

Before carrying out these studies, parameters important for the study design were established. The establishment of these parameters will be explained first, followed by a description of the results from Studies 1 and 2.

3.1 Establishment of parameters

In order to study a possible interference between DNA damage and the two DNA-repair pathways, NER and BER, careful establishment of appropriate genotoxic exposure levels and titration of associated DNA repair enzymes in the comet assay were essential to conduct.

First, optimal concentrations of the lesion-specific endonuclease-extracts (Fpg and T4endoV) used in our comet experiments were established, since the use of unnecessarily high concentrations of the extracts will give rise to unspecific DNA damage due to endonuclease activity.

Secondly, it was important to ensure that the induced lesion levels were within the dynamic detection range of the comet assay. It was therefore necessary to find the optimal dose of the different genotoxic exposures. In addition, the time-line of repair of each type of DNA damage had to be established to determine the optimal duration of repair incubations for each study.

Finally, both types of DNA damage (oxidative DNA lesions and helix-distorting DNA lesions) were to be present simultaneously in the cells during a significant time of the following repair period (see Figure 2.1). The level of interfering DNA damage should be in the upper part of the dynamic detection range of the comet assay to allow significant interfering DNA damage to be present during the time period repair was assessed.

3.1.1 Parameters for oxidative DNA lesions

3.1.1.1 Titration of Fpg-extract concentration

To determine the optimal concentration of Fpg-extract, a dose-response curve was established (Figure 3.1). Appropriately exposed samples of *Ogg1*$^{+/+}$ MEFs were treated with three different concentrations of the Fpg-extract or enzyme buffer alone. Oxidative lesions were introduced by treating the MEFs with the phototoxic compound Ro 12-9786 together with increasing doses of visible light. The level of DNA damage in unexposed cells without enzyme treatment (in majority revealing SSBs and alkali-labile sites and referred to as background damage level), were modest (close to 20 % DNA in the tail). The tail DNA intensity did not increase in the Ro 12-9786 plus light-exposed samples without enzyme treatment. An increasing Fpg-concentration resulted in three dose-response curves with increasing DNA damage levels from 20 % to about 80 % DNA in the tail. No induced oxidative lesions were apparent in the unexposed samples revealing low unspecific activity in this concentration range. The three dose response curves obtained were close to linear. In the dose response curve with Fpg-extract concentration of 0.01 µg/ml, generally lower damage levels were observed in all samples, indicating a sub-optimal Fpg-extract concentration and thus underestimating the Fpg-sensitive lesions. However, the 10 fold higher concentration of 0.1 µg/ml gave a non-linear curve, as this enzyme concentration revealed a damage level higher than expected at the light exposure dose of 3 min. Thus, the Fpg-extract concentration of 0.05 µg/ml was chosen for further experiments, as this concentration gave a dose response curve with an acceptable linearity.

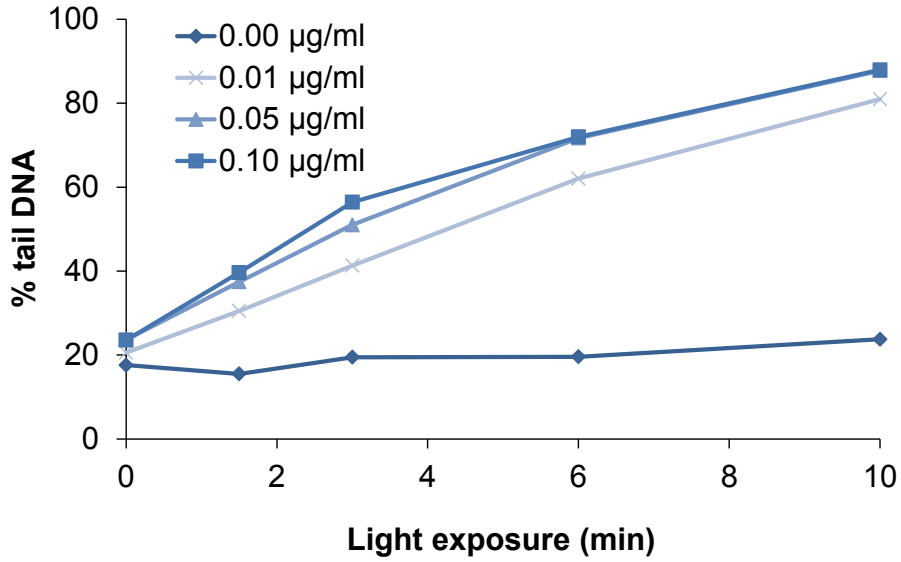

Figure 3.1: Titration of the Fpg-extract. A dose response curve of *Ogg1*$^{+/+}$ MEFs treated with the photosensitizer Ro 12-9786 (2 µM) and increasing doses of visible light (0, 1.5, 3, 6 and 10 min) was prepared. The DNA damage was analysed in the comet assay with increasing concentrations of Fpg-extract (0, 0.01, 0.05 and 0.1 µg/ml). DNA damage level is presented as % tail DNA. Mean of three technical replicates is shown.

3.1.1.2 Establishment of DNA damage levels and repair duration related to oxidative DNA lesions

For the induction of oxidative DNA lesions, two exposure scenarios were to be chosen; one scenario for the repair assessment in Study 2 and one scenario to induce interfering oxidative DNA lesions for the repair assessment of helix-distorting DNA lesions in Study 1 (Figure 2.1). In both studies, MEFs were pre-treated with Ro 12-9786 (2 µM) prior to light exposure. In Study 2, the 6 min visible light exposure was chosen for further experiments, as this dose induced a damage level below saturation (Figure 3.1) and the repair rate could thus be estimated. In the case of Study 1, it was decided to double the light exposure dose (i.e. 12 min light exposure instead of 6 min), as it was important to choose a sufficiently high dose of oxidative stress in order to sustain a relatively high level of interfering oxidative DNA lesions throughout the entire repair period for helix-distorting DNA lesions without introducing any cytotoxicity. It should be noted that the 12 min light exposure dose saturated the assay. However, this saturation is irrelevant, as only the detection of helix-distorting DNA lesions was critical.

In order to establish the optimal DNA repair time of oxidative DNA lesions in MEFs, cells were exposed to Ro 12-9786 and irradiated with light for 6 min before the cells were allowed

to repair the damage for 3 or 6 h. The induced damage should not be completely repaired; however the DNA damage level reduction should be considerable. An optimal reduction was observed after 3 h in the case of *Ogg1*$^{+/+}$ MEFs. However, the reduction was not as prominent in the *Ogg1*$^{-/-}$ MEFs, and hence a repair period of 6 h was chosen for the repair of oxidative DNA lesions in Study 2 (Figure 3.2.B and D). Background levels were generally low in the repair assessment studies (Figure 3.2.A and C).

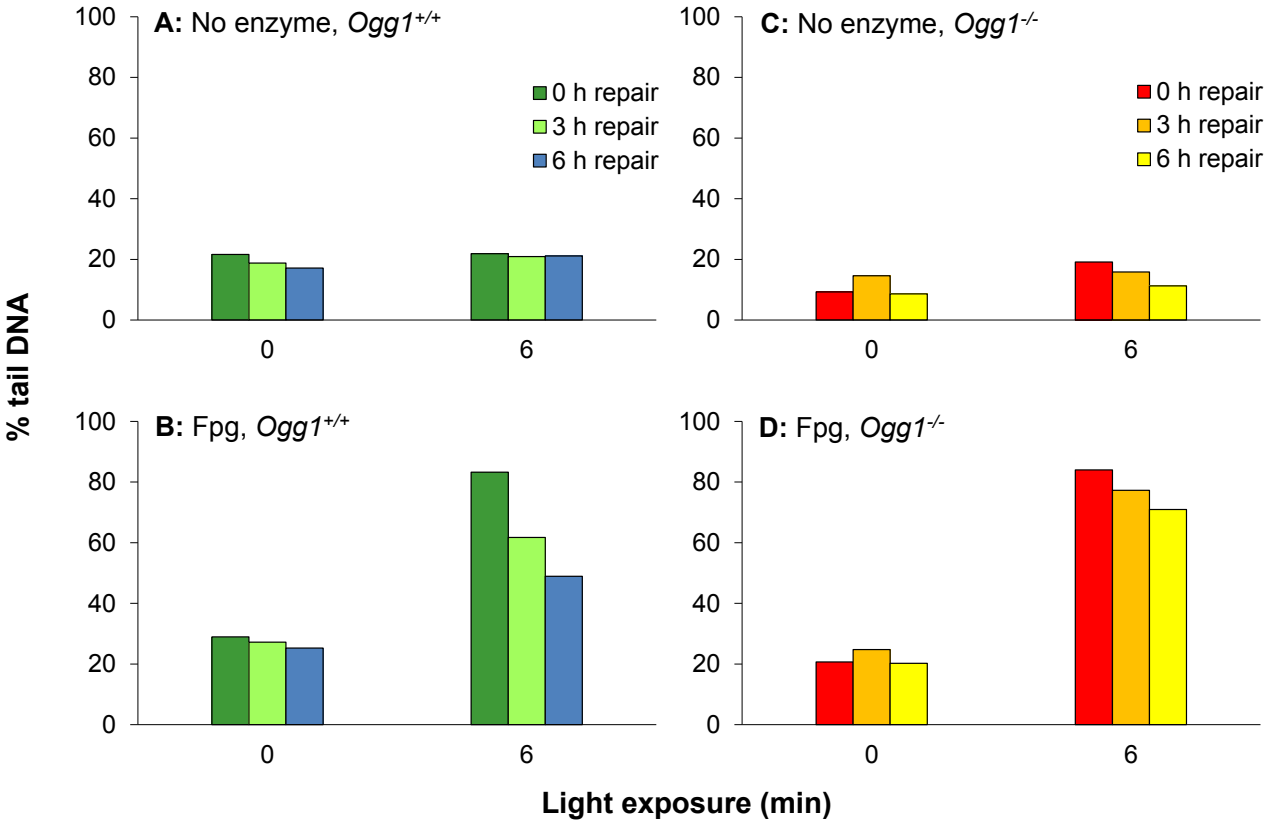

Figure 3.2: Establishment of repair duration of oxidative DNA lesions. MEFs exposed to light (0 or 6 min) in the presence of the photosensitizing agent Ro 12-9786 (2 µM) were allowed to repair for 0, 3 or 6 h (dark green, light green and blue bars, respectively, in the case of *Ogg1*$^{+/+}$ and red, orange and yellow bars, respectively, in the case of *Ogg1*$^{-/-}$). DNA damage was measured in the comet assay, with (B and D) or without (A and C) Fpg-extract treatment (0.05 µg/ml). DNA damage is presented as % tail DNA. Mean of three technical replicates is shown.

3.1.2 Parameters for helix-distorting DNA lesions

3.1.2.1 Titration of T4endoV-extract concentration

To determine the optimal concentration of T4endoV enzyme-extract, a dose response curve was established by irradiating HPBL with increasing doses of UVC. Irradiated cells were

treated with four different concentrations of the enzyme-extract (Figure 3.3). An untreated control was also included to detect any unspecific activity. HPBL was used as a substitute for MEFs in the case of the T4endoV-extract titration as these cells were easily available at the time when MEFs were infected with *Mycoplasma*.

The results clearly show that the damage level in cells without enzyme treatment was close to 0 % (a typical background damage for HPBL), regardless of UVC dose given. This was also the case for the level of background damage in the three dose response curves. Although being close to linear, the damage levels in the dose response curves from the two T4endoV-extract concentrations of 1.0 and 5.0 µg/ml were generally lower than the level for the other doses given. On the contrary, the higher concentrations (8.7 and 15 µg/ml) both revealed higher levels of damage. Since the extract concentration of 15.0 µg/ml revealed high levels of lesions at 0.5 and 1.0 J/m^2 without introducing any unspecific cleavage at 0 J/m^2, this concentration was chosen for further experiments.

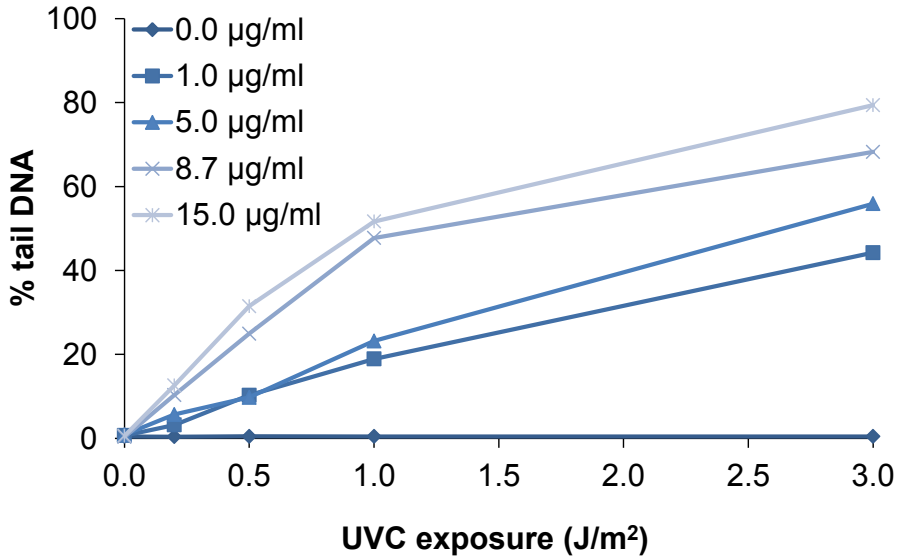

Figure 3.3: Titration of T4endoV-extract. A dose response curve of HPBL treated with increasing doses of UVC (0, 0.2, 0.5, 1.0 and 3.0 J/m^2) was prepared. The DNA damage was measured in the comet assay with increasing concentration of T4endoV-extract (0, 1.0, 5.0, 8.7 and 15 µg/ml). DNA damage level is presented as % tail DNA. Mean of three technical replicates is shown.

3.1.2.2 Establishment of DNA damage levels and repair duration related to UVC

UVC exposure was used for induction of the NER pathway. Experiments were conducted in order to establish an appropriate dose of UVC and further, to find the optimal duration for the

repair of these lesions. Two different doses of UVC radiation (0.5 and 1.0 J/m^2) were used, in addition to an unexposed control. The *Ogg1*$^{+/+}$ and *Ogg1*$^{-/-}$ MEFs were allowed to repair for 0, 8 and 16 h.

For the induction of helix-distorting DNA lesions, the UVC exposure dose of 0.5 J/m^2 was chosen for both Study 1 and Study 2. The reason for this was that helix-distorting DNA lesions take longer time to repair than oxidative DNA lesions, and thus the interfering helix-distorting DNA lesions were present throughout the entire repair period of oxidative DNA lesions in Study 2. The highest UVC dose (1.0 J/m^2) gave damage levels in the upper part of the dynamic detection range of the comet assay, both in *Ogg1*$^{+/+}$ and *Ogg1*$^{-/-}$ MEFs (Figure 3.4.B and D). Exposing to 0.5 J/m^2 gave a suitable damage level in the upper part of the dynamic detection range in order to follow repair. This dose was therefore chosen as the optimal dose in both studies.

For DNA repair assessment in Study 1, the reduction of the induced levels of helix-distorting DNA lesions were to be measured. The induced damage should not be completely repaired; however the DNA damage level reduction should be considerable. Such a reduction was not observed after 8 h, neither in *Ogg1*$^{+/+}$ (Figure 3.4.B) nor *Ogg1*$^{-/-}$ MEFs (Figure 3.4.D). After 16 h, however, the reduction was optimal in both cell types, and was therefore chosen as the repair time of helix-distorting DNA lesions in Study 1. Background damage levels were generally acceptable in the repair assessment experiment (Figure 3.4.A and C).

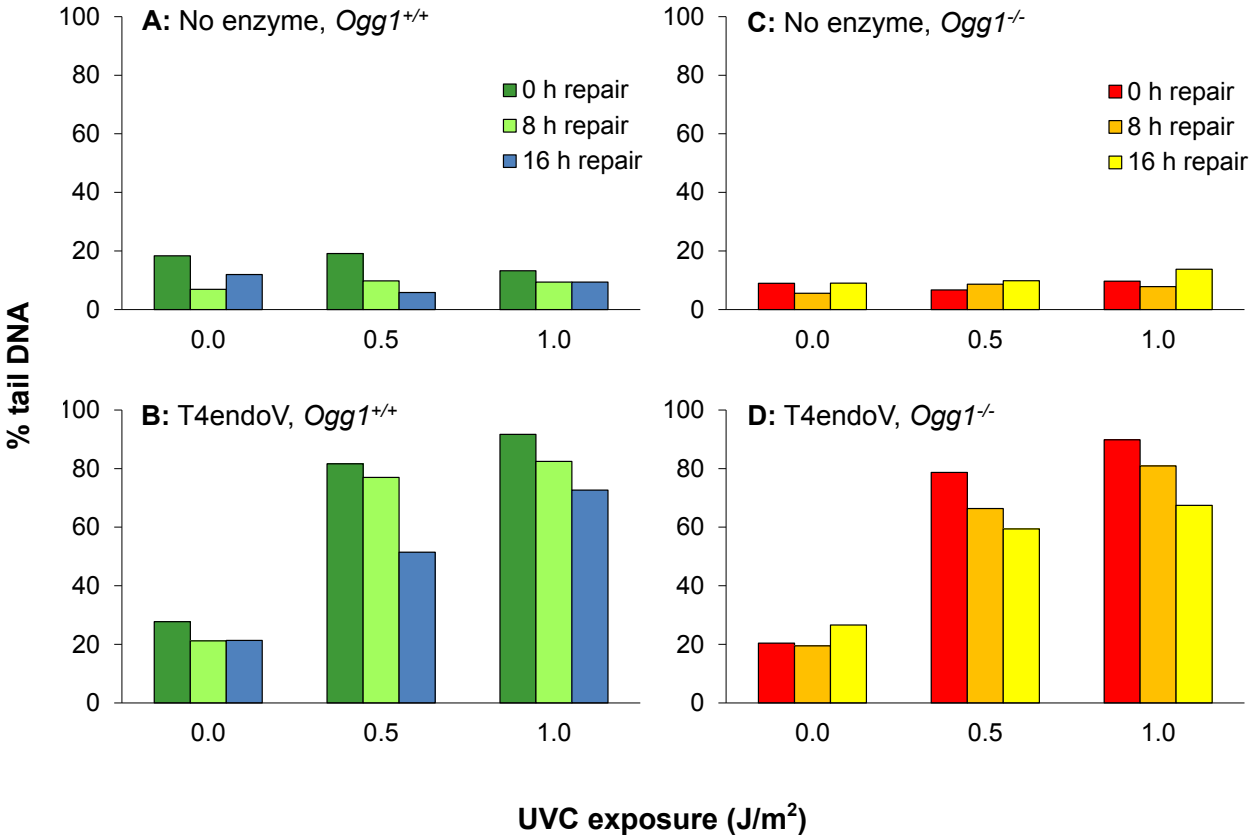

Figure 3.4: Establishment of DNA damage levels and repair duration of helix-distorting DNA lesions. MEFs irradiated with UVC (0.5 J/m^2 or 1.0 J/m^2) were allowed to repair for 0, 8 or 16 h (dark green, light green and blue bars, respectively, in the case of *Ogg1*$^{+/+}$ and red, orange and yellow bars, respectively, in the case of *Ogg1*$^{-/-}$). DNA damage was measured in the comet assay, with (B and D) or without (A and C) T4endoV-extract treatment (15 µg/ml). DNA damage is presented as % tail DNA. Mean of three technical replicates is shown.

3.2 Cell viability

3.2.1 Cytotoxicity

To make sure that the given doses during Ro 12-9786 plus light and UVC exposure in Study 1 and 2 did not exert cytotoxic effects, cytotoxicity assessment was conducted by means of the trypan blue exclusion test as described in section 2.5. The results from this assessment are presented in Table 3.1, and show that the viability of controls as well as exposed cells was similar, generally above 95 %. These results showed no induced cytotoxicity after the combined exposure both prior to and after the repair period.

Table 3.1: Cell viability*.

Repair time	*Ogg1*$^{+/+}$ MEFs Negative control (mean % viable cells ± SD)	*Ogg1*$^{+/+}$ MEFs Ro 12-9786 plus light and UVC (mean % viable cells ± SD)	*Ogg1*$^{-/-}$ MEFs Ro 12-9786 plus light and UVC (mean % viable cells ± SD)
0 h	98.2 ± 0.6	95.8 ± 0.6	96.9 ± 0.4
16 h	97.1 ± 0.2	97.1 ± 2.2	97.8 ± 1.8

*Per cent cell viability (mean of two replicate experiments) ± standard deviation (SD) of *Ogg1*$^{+/+}$ and *Ogg1*$^{-/-}$ MEFs assessed by trypan blue exclusion, at 0 and 16 h after exposure. The cells were exposed to Ro 12-9786 plus light and UVC. An unexposed negative control of *Ogg1*$^{+/+}$ MEFs was included.

3.2.2 *Mycoplasma*

The MEF cultures (*Ogg1*$^{-/-}$ and *Ogg1*$^{+/+}$) used for this study were tested for *Mycoplasma* once they arrived in our laboratory (from Department of Medical Biochemistry, Oslo University Hospital). Unfortunately, the first batch of MEFs that we received had to be discarded due to a positive *Mycoplasma* test. However, we received a new batch of both MEF cultures in early passages that were not infected with *Mycoplasma* (results not shown), and thus we were able to commence our study.

3.3 Role of low level oxidative stress on repair of helix-distorting DNA lesions

One of the aims of this project was to investigate whether low levels of oxidative stress perturbs repair of helix-distorting DNA lesions in embryonic fibroblasts from *Ogg1*$^{+/+}$ or *Ogg1*$^{-/-}$ mice (Study 1). The cells were exposed *in vitro* to the photosensitizing agent Ro 12-9786 (2 μM) plus visible light (12 min), followed by exposure to UVC (0.5 J/m^2). Two biological replicates were included for each treatment, one of which was harvested immediately after exposure, whereas the other one was harvested after 16 h of repair at 37 °C. Three controls were included for each repair period (0 and 16 h); an unexposed (negative) control, a control exposed to UVC and light and a control exposed to UVC and Ro 12-9786. Cells were moulded in three technical replicates onto three films subject to various enzyme treatment scenarios; one film was treated with T4endoV-extract to reveal UVC-induced DNA lesions, a second film was treated with Fpg-extract in order to reveal oxidative DNA lesions,

whereas the last film was an untreated control, which reveals strand breaks and alkali-labile sites only.

Unexpectedly, we observed a tendency of elevated levels of strand breaks (no enzyme treatment) in both *Ogg1*$^{+/+}$ and *Ogg1*$^{-/-}$ MEFs exposed to visible light together with UVC or visible light together with UVC and Ro 12-9786 prior to repair (Figure 3.5.A and D). The damage levels in MEFs exposed to both UVC and Ro 12-9786 in addition to visible light were approximately 1.5 times higher than the damage levels in cells exposed to UVC and light alone. The elevated levels of damage became a technical problem when calculating net T4endoV- or Fpg-sensitive sites. These sites are normally calculated by subtracting scores from non-enzyme treated cells from scores from enzyme treated cells. However, if the damage level in the samples without enzyme treatment is high, the reliability of the net sensitive site-results may be questioned. Consequently, the decision was to use total Fpg or T4endoV damage levels without subtracting the control level.

Importantly, we managed to sustain high levels of interfering oxidative lesions (Fpg sensitive sites together with SSBs) throughout the experiment in the sample exposed to Ro 12-9786 plus light and UVC together (Figure 3.5.C and F). Furthermore, we observed high initial levels of helix-distorting DNA lesions (T4endoV-specific lesions) in *Ogg1*$^{+/+}$ and *Ogg1*$^{-/-}$ MEFs in all UVC exposed cells prior to repair (Figure 3.5.B and E). The damage level observed in unexposed controls were low in all cases, and we found no differences in this damage level after repair, neither in *Ogg1*$^{+/+}$ nor *Ogg1*$^{-/-}$ MEFs.

Following repair, levels of helix-distorting DNA lesions were considerably lower than the initial levels, both in *Ogg1*$^{+/+}$ and *Ogg1*$^{-/-}$ MEFs (Figure 3.5.B and E). However, we did not observe any significant difference in the damage level in any of the exposed samples after repair within one cell type.

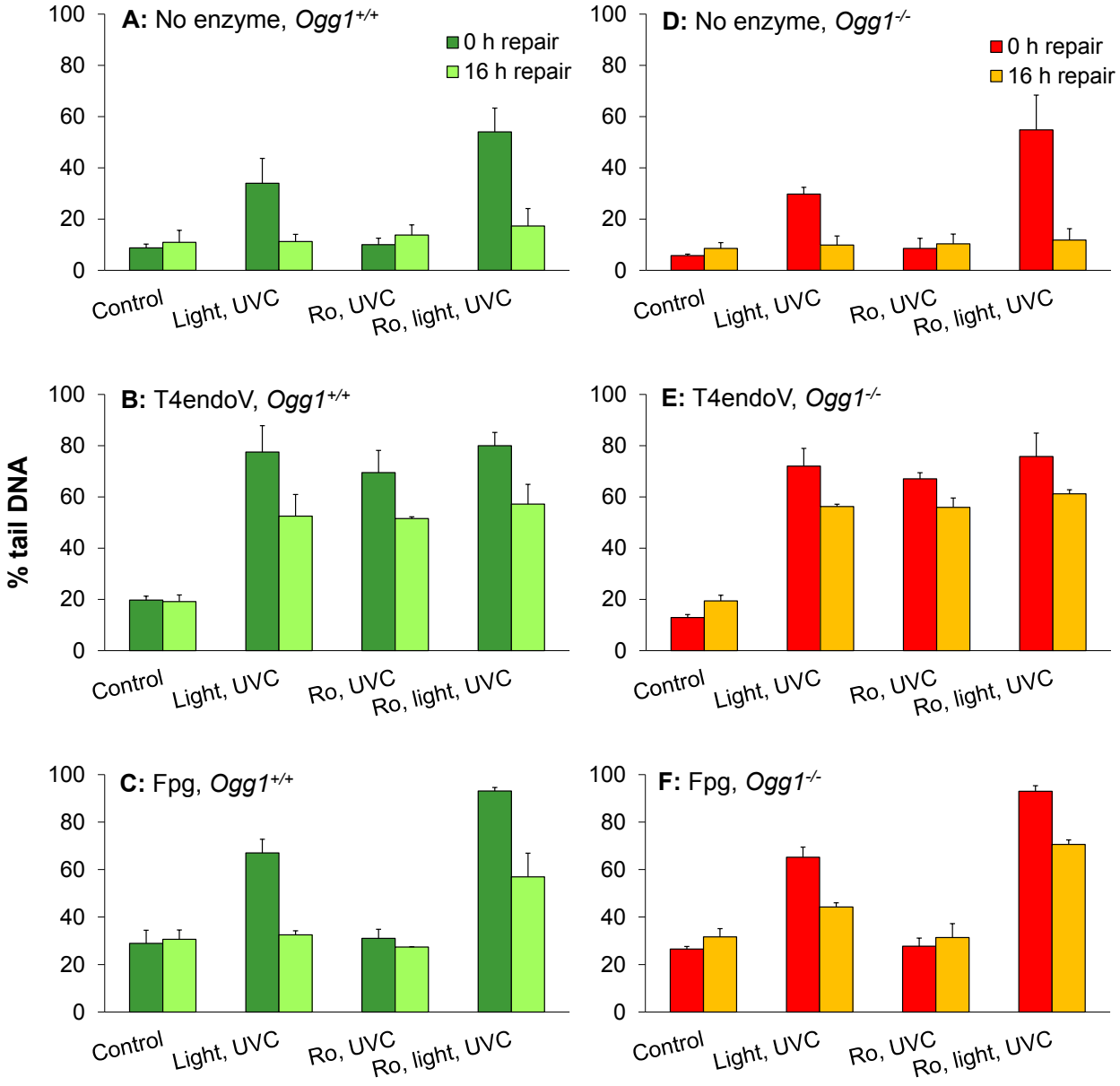

Figure 3.5: DNA repair of UVC-induced DNA lesions in mouse embryonic fibroblasts (MEFs) from *Ogg1*$^{+/+}$ and *Ogg1*$^{-/-}$ mice following a simultaneous single exposure to oxidative stress. DNA damage is measured in the comet assay in MEFs exposed to Ro 12-9786 (2 µm), light (12 min), and UVC (0.5 J/m^2), as indicated, before and after 16 h of repair. Tail DNA intensities (%) are presented of MEFs from *Ogg1*$^{+/+}$ (A-C) and *Ogg1*$^{-/-}$ (D-F) mice exposed to the following: Unexposed control; light and UVC; Ro 12-9786 and UVC; Ro 12-9786, light and UVC, in the respective order. Gels were incubated without enzyme-extract (A and D), with T4endoV-extract (B and E) or with Fpg-extract (C and F). The MEFs were harvested immediately after exposure (dark green and red bars) or following 16 h repair (light green and orange bars). The mean of two experiments is shown; each experiment is given as the mean of 100 scored comets on three replicate gels. In order to visualise differences between the two experiments, error bars representing the standard deviation are shown. Column charts of each experiment are shown in Appendix A, Figure A.1(*Ogg1*$^{+/+}$ MEFs) and Figure A.2 (*Ogg1*$^{-/-}$ MEFs).

The observed repair capacity in the samples exposed to Ro 12-9786 and UVC was slightly lower than the other two exposed samples (light + UVC and Ro 12-9786 + light + UVC, respectively), both in *Ogg1*$^{+/+}$ and *Ogg1*$^{-/-}$ MEFs (Figure 3.6.A and B). However, this difference was not significant.

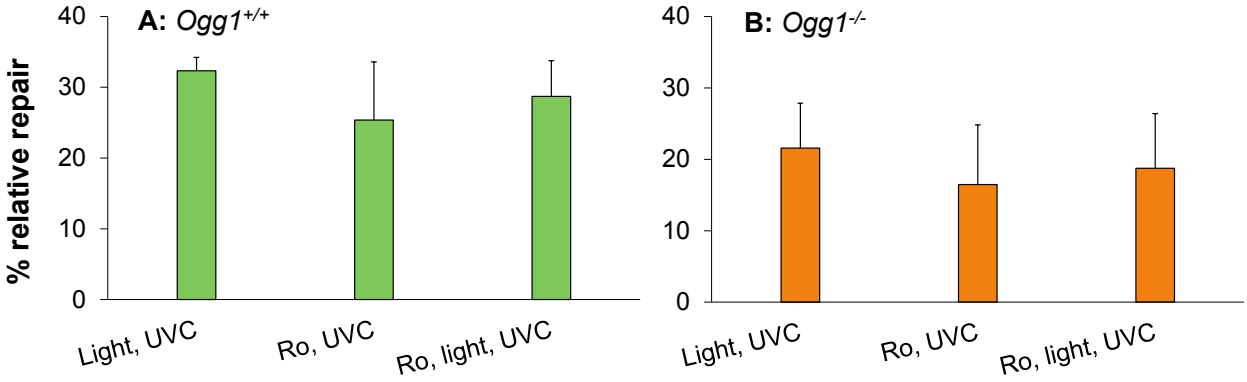

Figure 3.6: Relative repair of T4endoV-sensitive sites and SSBs. MEFs from *Ogg1*$^{+/+}$ (A) or *Ogg1*$^{-/-}$ (B) mice were exposed to Ro 12-9786, light (12 min) (2 µm) and UVC (0.5 J/m^2), as indicated. DNA damage was measured before and after 16 h of repair and relative repair (%) was calculated. The error bars represent the standard deviation between two separate experiments. Column charts of each experiment are shown in Appendix A, Figure A.3.A (*Ogg1*$^{+/+}$ MEFs) and B (*Ogg1*$^{-/-}$ MEFs).

3.4 Role of Ogg1 on the repair of helix-distorting DNA lesions

Next we wanted to study whether the DNA repair protein Ogg1 may influence the repair of helix-distorting DNA lesions in MEFs. This was investigated by comparing the relative repair of such lesions in *Ogg1*$^{+/+}$ and *Ogg1*$^{-/-}$ MEFs (Figure 3.6). As already mentioned before, we observed no significant difference in repair between the various exposed samples for each of the two cell types. Interestingly, when comparing the repair capacity of helix-distorting lesions between the two genotypes, we observed a clear difference. The repair of helix-distorting lesions in *Ogg1*$^{+/+}$ MEFs was more prone than in *Ogg1*$^{-/-}$, regardless of interfering oxidative damage level. One more experiment is needed in order to test whether the observed difference is statistically significant.

3.5 Role of helix-distorting DNA lesions on repair of oxidative DNA lesions

Another aim of this project was to investigate whether helix-distorting DNA lesions perturb repair of oxidative DNA lesions in embryonic fibroblasts from *Ogg1*$^{+/+}$ mice (Study 2). The cells were exposed *in vitro* to the photosensitizing agent Ro 12-9786 (2 µM) plus visible light (6 min), followed by exposure to UVC (0.5 J/m^2). Two biological replicas were included for each treatment, one of which was harvested immediately after exposure, whereas the other one was harvested after 6 h of repair at 37 °C. Three controls were included for each harvesting time; unexposed (negative) control cells to reveal any damage that may be introduced during cell preparation, a Ro 12-9786-exposed control to ensure no genotoxic stress from the Ro 12-9786 compound at 2µM and cells exposed to Ro 12-9786 plus light to ensure no additional T4endoV-specific damage induced by UVC in this sample. The gels containing DNA was treated with Fpg- or T4endoV-extracts in order to reveal oxidative lesions and UVC-induced lesions, respectively. Enzyme buffer controls (without endonuclease treatment) were also included. The samples without enzyme treatment showed low background damage levels (Figure 3.7.A). Thus, the "net" Fpg- and T4endoV-sensitive sites were calculated by subtracting the background damage level obtained after 'no enzyme' treatment from the damage level obtained after Fpg- or T4endoV-extract treatment.

As intended, we observed high levels of interfering helix-distorting lesions (T4endoV-sensitive sites) in the UVC exposed samples (Figure 3.7.C). The unexposed sample as well as the sample exposed to Ro 12-9786 only, showed low damage levels in all cases as expected. High initial levels of oxidative DNA lesions (Fpg-sensitive sites) (Figure 3.7.B) were found in both samples exposed to Ro 12-9786 plus light, regardless of additional UVC exposure. After 6 h of repair, there were still no differences in the level of oxidative DNA lesions between the Ro 12-9786 plus light exposed samples or the Ro 12-9786 plus light and UVC exposed samples, although the damage levels were considerably reduced (Figure 3.7.B).

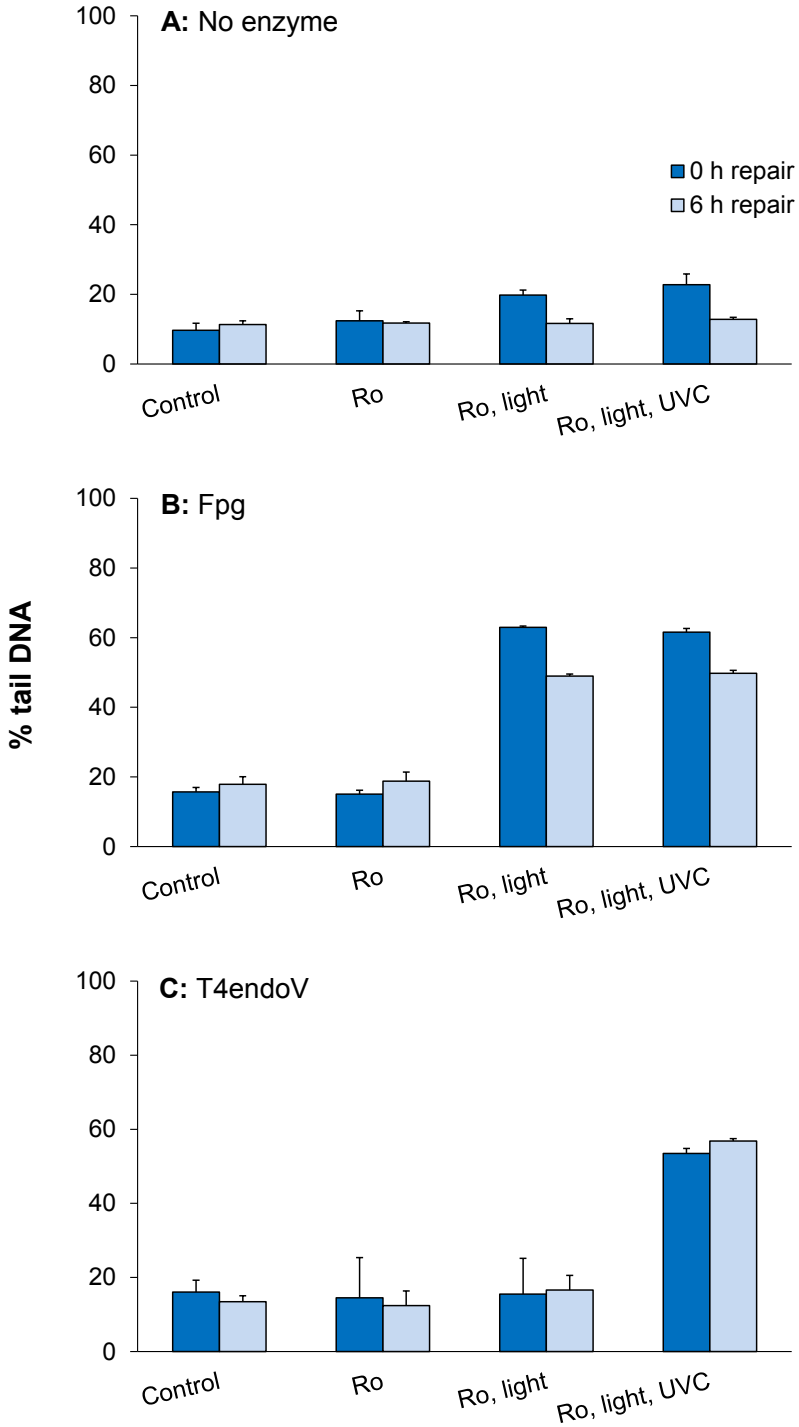

Figure 3.7: DNA repair of oxidative DNA lesions in mouse embryonic fibroblasts (MEFs) from *Ogg1*$^{+/+}$ mice following a simultaneous single exposure to UVC. DNA damage is measured in the comet assay in MEFs exposed to Ro 12-9786 (2 µm), light (6 min), and UVC (0.5 J/m^2), as indicated, before and after 6 h of repair. Tail DNA intensities (%) are presented of *Ogg1*$^{+/+}$MEFs exposed to the following: Unexposed control; Ro 12-9786; Ro 12-9786 and light; Ro 12-9786, light and UVC, in the respective order. Gels were incubated without enzyme-extract (A), with Fpg-extract (B) or with T4endoV-extract (C). The MEFs were harvested immediately after exposure (dark blue bars) or following 6 h repair (light blue bars). The mean of two experiments is shown; each experiment is given as the mean of 100 scored comets on three replicate gels. In order to visualise differences between experiments, error bars representing the standard deviation are shown. A column chart of each experiment is shown in Appendix A, Figure A.4.

Thus, no obvious difference in relative repair of oxidative lesions was observed even in the presence of helix-distorting DNA lesions, as seen in Figure 3.8.

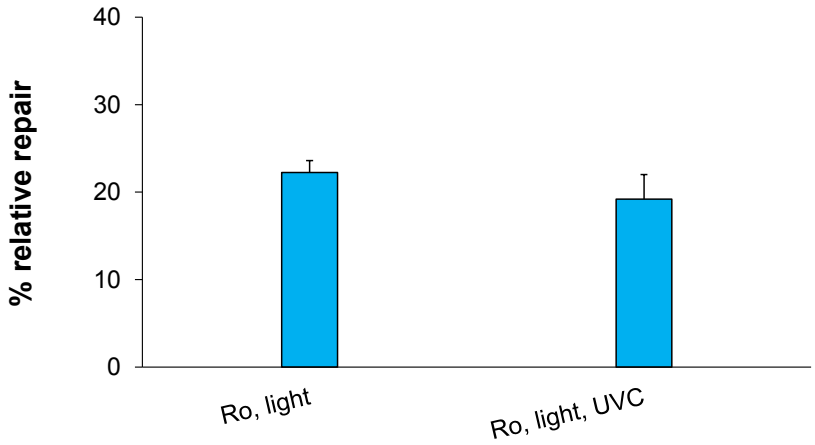

Figure 3.8: Relative repair of Fpg-sensitive sites. MEFs from *Ogg1*$^{+/+}$ mice were exposed to Ro 12-9786 (2 μm), light (6 min), and UVC (0.5 J/m^2), as indicated. DNA damage was measured before and after 6 h of repair and relative repair (%) was calculated. The error bars represent the standard deviation between two separate experiments. A column chart of each experiment is shown in Appendix A, Figure A.5.

4 DISCUSSION

The present study is divided into two parts; Study 1 and Study 2 (Figure 2.1).

In summary, the results from Study 1 suggest that a single low exposure to oxidative stress has no apparent effect on cellular repair of low levels of helix-distorting DNA lesions in MEF cells. On the other hand, the DNA repair protein Ogg1 appears to play a role on the repair of helix-distorting DNA lesions.

The results from Study 2 indicate that the presence of low levels of helix-distorting DNA lesions does not influence the repair of oxidative DNA lesions.

Before discussing these findings, some technical considerations will be addressed.

4.1 Technical considerations

In Study 1, we unexpectedly observed increased comet tail DNA intensities (SSBs and alkali-labile lesions), both in *Ogg1*$^{+/+}$ and *Ogg1*$^{-/-}$ MEFs, following an initial 12 min exposure to visible light followed by 0.5 J/m^2 of UVC, independent of the presence of Ro 12-9786 (Figure 3.5.A and D). If this observation was to follow a linear relationship, one would expect increased, however lower, tail DNA intensities after 6 min of visible light exposure. However, this is not the case. There may be several possible explanations to this observation.

A tungsten-halogen lamp enabling simultaneous exposure of multiple samples was used for visible light exposure in the present study. Unfortunately, this lamp produces heat. Increased temperature is known to increase enzyme reaction rates, which may thereby increase the enzyme activities of cellular endonucleases (Daniel *et al.*, 2003). Such enzymes can convert already existing DNA lesions into SSBs; a problem that could be circumvented by exposing samples to cold visible light sources. However, the cold visible light lamp in our lab had restricted suitability for this study since it can only be used for exposing very few samples simultaneously. Instead, the cell samples were kept on a precooled metal plate during the exposure to visible light in order to avoid increased temperatures. It is therefore likely that the temperature did not increase sufficiently for a significant increase in endonuclease activities to take place during the first six min of exposure. However, such an increase in temperature may have occurred between six and 12 min of visible light exposure.

Since the increases in comet tail DNA intensities were limited to cells exposed to visible light followed by UVC, it can be speculated that there is a relationship between the increased damage levels and the order and combination of exposure to visible light and UVC. This exact order of exposure was chosen to avoid formation of alkali-sensitive Dewar isomers, which would appear as SSBs in the comet assay (as described in section 2.2.3). The speculation of a relationship between the exposure scenario and induced DNA damage levels is supported by findings in preliminary experiments, where no increases in tail DNA intensities were observed after separate exposures of MEFs to 10 min of visible light or to 0.5 J/m^2 of UVC alone (Figure 3.1 and Figure 3.4.A and C, respectively).

However, as the cells were exposed to visible light and UVC in growth medium, there is a possibility that components of the growth medium may participate in the formation of DNA damage detectable in the comet assay. This may have occurred by photoconversion of medium components by visible light and further photoactivation by UVC. For instance, benzylpenicillin, an antibiotic present in our growth medium, generate ROS upon exposure to sunlight and all three subtypes of UV (Ray *et al.*, 1996). Other possible components that could be photoconverted are the proteins originating from FCS present in the medium.

The increased comet tail DNA intensities in cells exposed to visible light and UVC did not seem to influence the repair rates observed with respect to T4endoV-sensitive DNA lesions, since the decline in T4endoV-sensitive DNA lesions was similar in MEF cells exposed to Ro 12-9786 plus UVC (Figure 3.5.B and E, 3rd group of columns, light green and orange column, respectively) compared with MEFs exposed to visible light plus UVC or Ro12-9786, visible light plus UVC (Figure 3.5.B and E, 2nd and 4th groups of columns, light green and orange column, respectively).

4.2 Effect of oxidative stress on NER

Based upon studies by Langie and co-workers (Langie *et al.*, 2007; Langie *et al.*, 2010), which showed a clear relationship between oxidative stress and reduced NER capacity in cellular extracts, *in vitro* as well as *in vivo*, we aimed to investigate whether oxidative stress can perturb the cellular repair of helix-distorting DNA lesions in MEFs in a defined *in vitro* system.

The present study suggests that a single low-dose exposure of oxidative stress does not perturb the repair of low-dose levels of helix-distorting DNA lesions, neither in *Ogg1*$^{+/+}$ MEFs nor *Ogg1*$^{-/-}$ MEFs (Figure 3.6). Several explanations can be envisioned:

Low levels of oxidative stress and ROS-generated oxidative DNA lesions were induced. These levels may be below a certain threshold level for inhibition of DNA repair. The dose levels were chosen in relation to the maximal detection level of the comet assay. However, it is still possible, and also likely, that chronic exposures causing a continuous attack of proteins, membranes and DNA, or merely higher doses of ROS do perturb the repair of helix-distorting DNA lesions, as suggested by Langie and co-workers when assessing repair activities in cellular extracts (Langie *et al.*, 2007; Langie *et al.*, 2010).

In our study, oxidative DNA lesions were induced by a single dose of oxidative stress. However, if we would have exposed cells repeatedly, i.e. generating chronic oxidative stress, we would gain sustained levels of oxidative DNA lesions. Such increased oxidative stress has previously been demonstrated to inhibit NER, both *in vitro* and *in vivo* (Langie *et al.*, 2007; Langie *et al.*, 2010). In the *in vitro* study, acute inhibition of NER capacities in cellular extracts were observed after exposure of A549 human pulmonary epithelial cells to high doses of oxidative stress (100 μM of the oxidizing agent hydrogen peroxide (H_2O_2) for 1 h). Although this exposure was not chronic, the oxidative stress in the cells was sustained by depletion of the endogenous antioxidant glutathione (GSH) prior to H_2O_2 exposure (Langie *et al.*, 2007). This result was later followed up *in vivo*, where an intramuscular injection of iron (200 mg) given at day three after birth caused chronic oxidative stress and inhibition of NER capacity in cell extracts from the colon of new-born piglets. This inhibition was reversible by antioxidant supplementation, confirming that oxidative stress was involved in the inhibition (Langie *et al.*, 2010). However, it should be noted that the *in vitro* study by Langie *et al.* (2007) differs from our study with respect to the induction of oxidative stress, which in their case was done by means of H_2O_2. Unlike Ro 12-9786 and visible light, H_2O_2 induces SSBs in addition to oxidative DNA lesions, and H_2O_2 will attack membrane lipids more aggressively than the other two agents. It can be speculated that the SSBs may contribute to the inhibition of NER, or that lipid peroxidation products inhibit NER (Güngör *et al.*, 2010b). Moreover, measurements of NER capacity in the studies by Langie and Güngör and co-workers (Güngör *et al.*, 2007; Güngör *et al.*, 2010a; Güngör *et al.*, 2010b; Langie *et al.*, 2006; Langie *et al.*, 2007; Langie *et al.*, 2010) were based on the capacity of cell/tissue extracts to incise DNA with helix-distorting lesions in a modified version of the comet assay (Langie *et al.*, 2006), as

opposed to our measurements of cellular repair capacities. In cell/tissue extracts, repair enzymes are evenly distributed and withdrawn from their natural location in the cell, as opposed to cells in culture, where the repair enzymes may be confined to certain compartments of the cell, which is likely to influence their local availability for repair of damaged DNA.

Furthermore, neither of the studies by Langie and co-workers revealed a clear mode-of-action for the observed inhibition of NER. However, the effect of GSH-depletion (*in vitro*) and antioxidant supplementation (*in vivo*) on NER capacity supports the suspicion of a direct ROS-mediated inactivation of NER proteins being responsible for the inhibition rather than the existence of oxidative DNA lesions themselves. This suspicion is strengthened by the present findings of no inhibition of NER after simultaneously exposure to oxidative lesions, neither in *Ogg1*$^{+/+}$ nor *Ogg1*$^{-/-}$ MEFs. In *Ogg1*$^{-/-}$ MEFs, we expected higher spontaneous levels of 8-oxoG compared to *Ogg1*$^{+/+}$ MEFs. However, only small differences between the genotypes were observed with respect to Fpg-sensitive DNA lesion levels.

Due to the study design in the present study it was not possible to conclude on the discrepant results on possible inhibition of NER after oxidative stress. In further studies, it would be useful to investigate the importance of antioxidant status by GSH-depletion of MEFs prior to exposure to oxidative stress. Another interesting approach to obtain continuous oxidative stress is to utilize activated neutrophils. When activated by exposure to invading microorganisms, neutrophils generate ROS (for the purpose of killing the pathogen) (Babior *et al.*, 1973). Güngör *et al.* (Güngör *et al.*, 2007) observed a significant reduction of NER-activity in extracts from human alveolar epithelial cells (A549) *in vitro* following co-culturing with activated neutrophils. This finding was later confirmed *in vivo* (Güngör *et al.*, 2010a), where a relationship between lung inflammation and reduced pulmonary NER-activity was revealed. The basis of this NER reduction, and also the basis of neutrophil-induced genotoxicity, was later suggested to be formation of hypochlorous acid (HOCl) giving rise to various DNA lesions, including helix-distorting DNA lesions, via lipid peroxidation (Güngör *et al.*, 2010b). The formation of HOCl is catalysed by myeloperoxidase (MPO), a protein released by neutrophils upon activation (Güngör *et al.*, 2010b).

4.3 Role of Ogg1 in repair of helix-distorting DNA lesions

In order to study whether accumulated levels of 8-oxoG inhibit NER capacity, we compared repair capacities of *Ogg1*$^{-/-}$ and *Ogg1*$^{+/+}$ MEFs (Figure 3.6.A and B, respectively). Interestingly, the present study revealed more efficient repair of helix-distorting DNA lesions in *Ogg1*$^{+/+}$ MEFs compared to *Ogg1*$^{-/-}$ MEFs, regardless of level of accumulated oxidative DNA lesions. The differences are probably underestimated since the proliferative rate is 2:1 between *Ogg1*$^{-/-}$ and *Ogg1*$^{+/+}$ cells, respectively, leading to a more extensive dilution of the DNA damage in *Ogg1*$^{-/-}$ cells due to cell division alone. This finding suggests that the repair protein Ogg1 may play a role in the repair of helix-distorting DNA lesions.

This finding is substantiated by a previous finding in our lab of liver cells from Big Blue® *Ogg1*$^{-/-}$ mice displaying a considerable delayed removal of BPDE DNA-adducts following *in vivo* exposure to B[a]P (Olsen, A. K., pers. comm., April 2012). However, it should be noted that B[a]P, when metabolized, may induce oxidative stress, with potential to influence NER repair efficiency (Langie *et al.*, 2007; Langie *et al.*, 2010).

Moreover, crosstalk between repair mechanisms do exist; xeroderma pigmentosum, complementation group C (XPC), a protein involved in NER, has been showed to play an unexpected role in the removal of oxidative DNA lesions, most likely by acting as a co-factor in Ogg1-initiated BER (D'Errico *et al.*, 2006). The crosstalk between NER and BER may act in both directions in such a way that NER is perturbed in the absence of Ogg1.

4.4 Effect of helix-distorting DNA lesions on BER

In this part of the study, we investigated whether helix-distorting DNA lesions play a role for repair of oxidative DNA lesions. The study showed that in our experimental design, sustaining low levels of helix-distorting DNA lesions do not perturb repair of low-dose oxidative DNA lesions in *Ogg1*$^{+/+}$ MEFs (Figure 3.8).

Many environmental compounds are known to induce bulky helix-distorting DNA lesions as well as leading directly or indirectly to increased ROS production. Furthermore, in real-life we are often exposed to several agents simultaneously and conditions such as autoimmune diseases and chronic inflammations lead to increased ROS production. Moreover, UVC-radiation induces damage (such as CPDs) to pyrimidines (cytosine and thymine), whereas ROS attack mainly purines (adenine and guanine) but also to a lower degree pyrimidines. Induction of DNA lesions via several sources may lead to DNA lesions that are in proximity

to each other which is a challenge to the DNA repair systems without generating errors or strand breaks. Inhibition of repair is a logic outcome due to increased time requirements to resolve these challenges. Bergeron *et al.* (Bergeron *et al.*, 2010) showed that one of the major products of DNA oxidation, 8-oxoG, is refractory to excision by DNA glycosylases when it is involved in tandem DNA lesions (two lesions formed on adjacent nucleotides). In addition, helix-distorting DNA lesions may lead to steric interference in the removal of oxidative DNA lesions by BER. The induction of DNA damage is a largely stochastic event. Nonetheless, induction of DNA lesions often de-stabilises the DNA helix, making the DNA more susceptible to other DNA damaging agents.

4.5 Conclusions

The experimental results strongly suggest, that, in our experimental design:

- Sustaining low levels of helix-distorting DNA lesions do not perturb the repair of low-dose oxidative DNA lesions in wild type MEFs ($Ogg1^{+/+}$).
- Sustained oxidative DNA lesions, induced by a single initial exposure to oxidative stress, do not perturb the repair of low doses of helix-distorting DNA lesions, neither in wild type MEFs ($Ogg1^{+/+}$) nor in $Ogg1^{-/-}$ MEFs.
- The absence of the Ogg1 repair function seems to decrease the efficiency of repair of helix-distorting DNA lesions, regardless of the level of oxidative DNA lesions, suggesting that the BER-related repair protein Ogg1 plays a role in NER.
- The data therefore suggest that specific repair deficiencies rather than the presence of different types of lesions contribute to increased sensitivities of cells to combinations of exogenous and endogenous agents.
- Considering the significant role of DNA damage and its repair in health and disease, further studies should be carried out to clarify the link between oxidative stress and DNA lesions. Their influence on different DNA repair pathways as well as identification of crosstalks between DNA repair proteins/pathways should be characterised.

REFERENCES

Ames, B. N. (1989). Endogenous oxidative DNA damage, aging, and cancer. *Free radical research communications* **7**, 121-128.

Babior, B. M., Kipnes, R. S., and Curnutte, J. T. (1973). Biological defense mechanisms. The production by leukocytes of superoxide, a potential bactericidal agent. *Journal of Clinical Investigation* **52**, 741-744.

Bergeron, F., Auvré, F., Radicella, J. P., and Ravanat, J. L. (2010). $HO^{\bullet}$ radicals induce an unexpected high proportion of tandem base lesions refractory to repair by DNA glycosylases. *Proceedings of the National Academy of Sciences* **107**, 5528-5533.

Cleaver, J. E. (1989). DNA repair in man. *Birth defects original article series* **25**, 61-82.

Collins, A. R., Oscoz, A. A., Brunborg, G., Gaivão, I., Giovannelli, L., Kruszewski, M., Smith, C. C., and Štetina, R. (2008). The comet assay: topical issues. *Mutagenesis* **23**, 143-151.

Collins, A. R., Cadet, J., Möller, L., Poulsen, H. E., and Viña, J. (2004). Are we sure we know how to measure 8-oxo-7,8-dihydroguanine in DNA from human cells? *Archives of Biochemistry and Biophysics* **423**, 57-65.

Cooke, M. S., Evans, M. D., Dizdaroglu, M., and Lunec, J. (2003). Oxidative DNA damage: mechanisms, mutation, and disease. *The FASEB journal* **17**, 1195-1214.

D'Errico, M., Parlanti, E., Teson, M., de Jesus, B. M. B., Degan, P., Calcagnile, A., Jaruga, P., Bjørås, M., Crescenzi, M., and Pedrini, A. M. (2006). New functions of XPC in the protection of human skin cells from oxidative damage. *The EMBO journal* **25**, 4305-4315.

Daniel, R. M., Dunn, R. V., Finney, J. L., and Smith, J. C. (2003). The role of dynamics in enzyme activity. *Annual review of biophysics and biomolecular structure* **32**, 69-92.

De Bont, R., and van Larebeke, N. (2004). Endogenous DNA damage in humans: a review of quantitative data. *Mutagenesis* **19**, 169-185.

Duale, N., Olsen, A. K., Christensen, T., Butt, S. T., and Brunborg, G. (2010). Octyl Methoxycinnamate Modulates Gene Expression and Prevents Cyclobutane Pyrimidine Dimer Formation but not Oxidative DNA Damage in UV-Exposed Human Cell Lines. *Toxicological Sciences* **114**, 272-284.

Evans, M. D., Dizdaroglu, M., and Cooke, M. S. (2004). Oxidative DNA damage and disease: induction, repair and significance. *Mutation Research/Reviews in Mutation Research* **567**, 1-61.

Ferguson, L. R. (2010). Chronic inflammation and mutagenesis. *Mutation Research/Fundamental and Molecular Mechanisms of Mutagenesis* **690**, 3-11.

Floyd, R. A. (1990). Role of oxygen free radicals in carcinogenesis and brain ischemia. *The FASEB journal* **4**, 2587-2597.

Friedberg, E. C., Ganesan, A. K., and Seawell, P. C. (1980). [25] Purification and properties of a pyrimidine dimer-specific endonuclease from *E. coli* infected with bacteriophage T4. *Methods in Enzymology* **65**, 191-201.

Gillet, L. C. J., and Schärer, O. D. (2005). Molecular Mechanisms of Mammalian Global Genome Nucleotide Excision Repair. *Chemical Reviews* **106**, 253-276.

Gocke, E., Albertini, S., Chetelat, A. A., Kirchner, S., and Muster, W. (1998). The photomutagenicity of fluoroquinolones and other drugs. *Toxicology letters* **102**, 375-381.

Güngör, N., Godschalk, R. W. L., Pachen, D. M., van Schooten, F. J., and Knaapen, A. M. (2007). Activated neutrophils inhibit nucleotide excision repair in human pulmonary epithelial cells: role of myeloperoxidase. *The FASEB journal* **21**, 2359-2367.

Güngör, N., Haegens, A., Knaapen, A. M., Godschalk, R. W. L., Chiu, R. K., Wouters, E. F. M., and van Schooten, F. J. (2010a). Lung inflammation is associated with reduced pulmonary nucleotide excision repair in vivo. *Mutagenesis* **25**, 77-82.

Güngör, N., Knaapen, A. M., Munnia, A., Peluso, M., Haenen, G. R., Chiu, R. K., Godschalk, R. W. L., and van Schooten, F. J. (2010b). Genotoxic effects of neutrophils and hypochlorous acid. *Mutagenesis* **25**, 149-154.

Hansen, S. H., Olsen, A. K., Søderlund, E. J., and Brunborg, G. (2010). In vitro investigations of glycidamide-induced DNA lesions in mouse male germ cells and in mouse and human lymphocytes. *Mutation Research/Genetic Toxicology and Environmental Mutagenesis* **696**, 55-61.

Houtgraaf, J. H., Versmissen, J., and van der Giessen, W. J. (2006). A concise review of DNA damage checkpoints and repair in mammalian cells. *Cardiovascular Revascularization Medicine* **7**, 165-172.

Ide, H., and Kotera, M. (2004). Human DNA glycosylases involved in the repair of oxidatively damaged DNA. *Biological & pharmaceutical bulletin* **27**, 480-485.

Kamijo, T., Zindy, F., Roussel, M. F., Quelle, D. E., Downing, J. R., Ashmun, R. A., Grosveld, G., and Sherr, C. J. (1997). Tumor Suppression at the Mouse INK4a Locus Mediated by the Alternative Reading Frame Product p19 ARF. *Cell* **91**, 649-659.

Klaassen, C. D. (2001). Casarett and Doull's Toxicology - The Basic Science of Poisons, 6th edition. *McGraw-Hill,* New York, USA.

Klungland, A., Rosewell, I., Hollenbach, S., Larsen, E., Daly, G., Epe, B., Seeberg, E., Lindahl, T., and Barnes, D. E. (1999). Accumulation of premutagenic DNA lesions in mice defective in removal of oxidative base damage. *Proceedings of the National Academy of Sciences* **96**, 13300-13305.

Krokan, H. E., Nilsen, H., Skorpen, F., Otterlei, M., and Slupphaug, G. (2000). Base excision repair of DNA in mammalian cells. *FEBS letters* **476**, 73-77.

Krokan, H. E., Standal, R., and Slupphaug, G. (1997). DNA glycosylases in the base excision repair of DNA. *Biochemical Journal* **325**, 1-16.

Langie, S. A. S., Knaapen, A. M., Brauers, K. J. J., Van Berlo, D., Van Schooten, F. J., and Godschalk, R. W. L. (2006). Development and validation of a modified comet assay to phenotypically assess nucleotide excision repair. *Mutagenesis* **21**, 153-158.

Langie, S. A. S., Knaapen, A. M., Houben, J. M. J., van Kempen, F. C., de Hoon, J. P. J., Gottschalk, R. W. H., Godschalk, R. W. L., and Van Schooten, F. J. (2007). The role of glutathione in the regulation of nucleotide excision repair during oxidative stress. *Toxicology letters* **168**, 302-309.

Langie, S. A. S., Kowalczyk, P., Tudek, B., Zabielski, R., Dziaman, T., Olinski, R., Van Schooten, F. J., and Godschalk, R. W. L. (2010). The effect of oxidative stress on nucleotide-excision repair in colon tissue of newborn piglets. *Mutation Research/Genetic Toxicology and Environmental Mutagenesis* **695**, 75-80.

Lovell, D. P., and Omori, T. (2008). Statistical issues in the use of the comet assay. *Mutagenesis* **23**, 171-182.

Lowe, S. W., Jacks, T., Housman, D. E., and Ruley, H. E. (1994). Abrogation of oncogene-associated apoptosis allows transformation of p53- deficient cells. *Proceedings of the National Academy of Sciences of the United States of America* **91**, 2026-2030.

Missura, M., Buterin, T., Hindges, R., Hübscher, U., Kaspárková, J., Brabec, V., and Naegeli, H. (2001). Double-check probing of DNA bending and unwinding by XPA–RPA: an architectural function in DNA repair. *The EMBO journal* **20**, 3554-3564.

Mitchell, D. L., and Nairn, R. S. (1989). The biology of the (6-4) photoproduct. *Photochemistry and photobiology* **49**, 805-819.

Olsen, A. K., Duale, N., Bjørås, M., Larsen, C. T., Wiger, R., Holme, J. A., Seeberg, E. C., and Brunborg, G. (2003). Limited repair of 8–hydroxy-7,8-dihydroguanine residues in human testicular cells. *Nucleic acids research* **31**, 1351-1363.

Olsen, A. K., Lindeman, B., Wiger, R., Duale, N., and Brunborg, G. (2005). How do male germ cells handle DNA damage? *Toxicology and Applied Pharmacology* **207**, 521-531.

Ostling, O., and Johanson, K. J. (1984). Microelectrophoretic study of radiation-induced DNA damages in individual mammalian cells. *Biochemical and Biophysical Research Communications* **123**, 291-298.

Ray, R. S., Mehrotra, S., Prakash, S., and Joshi, P. C. (1996). Ultraviolet radiation-induced production of superoxide radicals by selected antibiotics. *Drug and chemical toxicology* **19**, 121-130.

Schneider, J. E., Price, S., Maidt, L., Gutteridge, J. M. C., and Floyd, R. A. (1990). Methylene blue plus light mediates 8-hydroxy 2'-deoxyguanosine formation in DNA preferentially over strand breakage. *Nucleic acids research* **18**, 631-635.

Singh, N. P., McCoy, M. T., Tice, R. R., and Schneider, E. L. (1988). A simple technique for quantitation of low levels of DNA damage in individual cells. *Experimental cell research* **175**, 184-191.

Sinha, R. P., and Häder, D. P. (2002). UV-induced DNA damage and repair: a review. *Photochemical & Photobiological Sciences* **1**, 225-236.

Steinman, H. A., Sluss, H. K., Sands, A. T., Pihan, G., and Jones, S. N. (2004). Absence of p21 partially rescues Mdm4 loss and uncovers an antiproliferative effect of Mdm4 on cell growth. *Oncogene* **23**, 303-306.

Taylor, J. S., Lu, H. F., and Kotyk, J. J. (1990). Quantitative conversion of the (6-4) photoproduct of TpdC to its Dewar valence isomer upon exposure to simulated sunlight. *Photochemistry and photobiology* **51**, 161-167.

Watson, J. D., Baker, T. A., Bell, S. P., Gann, A., Levine, M., and Losick, R. (2008). Molecular Biology of the Gene, 6th edition. *Cold Spring Harbor Laboratory Press,* New York, USA.

Yasuda, S., and Sekiguchi, M. (1970). T4 Endonuclease Involved in Repair of DNA. *Proceedings of the National Academy of Sciences* **67**, 1839-1845.

APPENDIX A

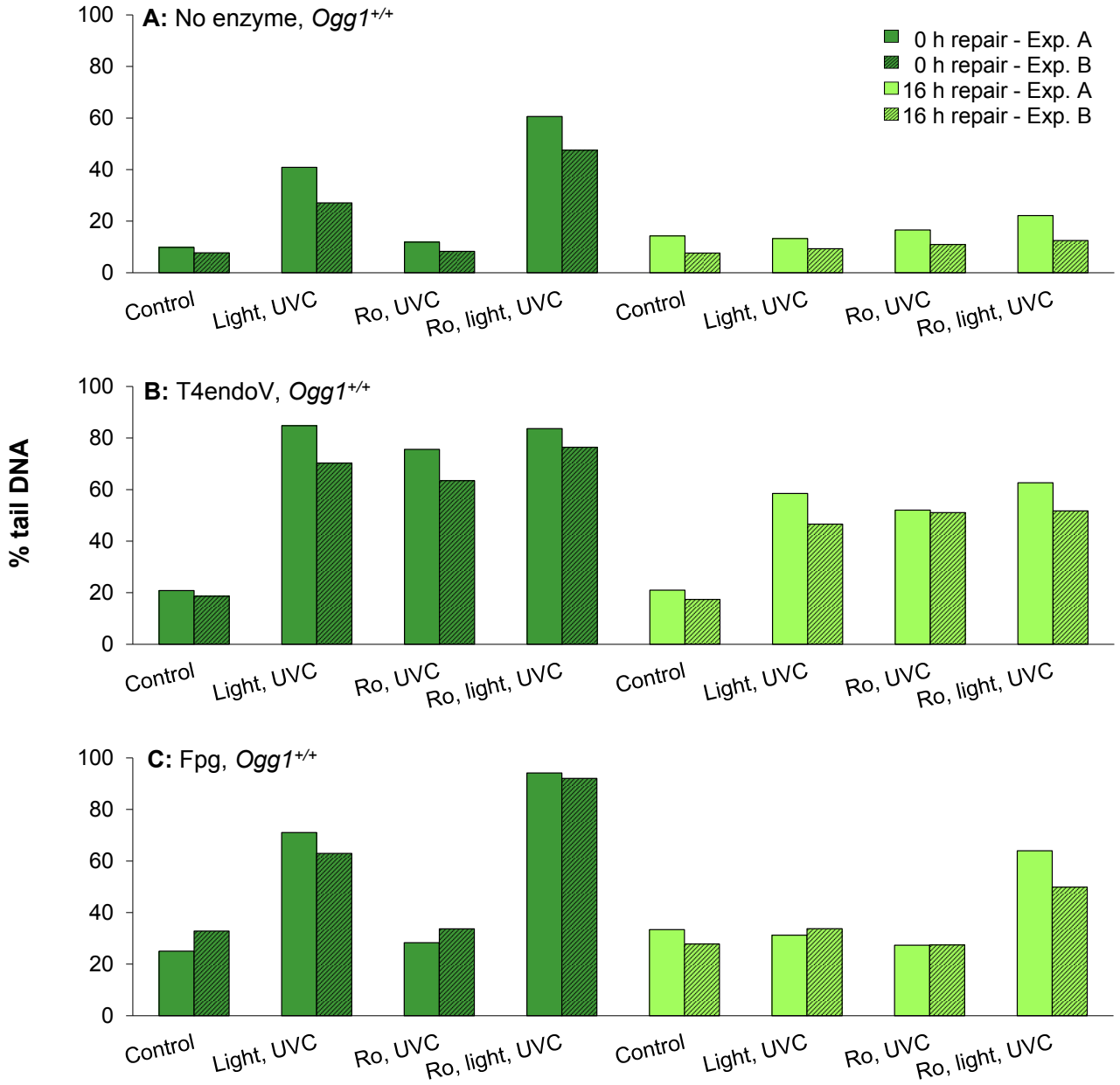

Figure A.1: DNA repair of UVC-induced DNA lesions in mouse embryonic fibroblasts (MEFs) from *Ogg1*$^{+/+}$ mice following a simultaneous single exposure to oxidative stress. DNA damage is measured in the comet assay in MEFs exposed to Ro 12-9786 (2 μm), light (12 min), and UVC (0.5 J/m^2), as indicated, before and after 16 h of repair. Tail DNA intensities (%) are presented of *Ogg1*$^{+/+}$MEFs exposed to the following: Unexposed control; light and UVC; Ro and UVC; Ro, light and UVC, in the respective order. Gels were incubated without enzyme-extract (A), with T4endoV-extract (B) or with Fpg-extract (C). The MEFs were harvested immediately after exposure (dark green bars) or following 16 h repair (light green bars). Two experiments are shown (Exp. A; full bars, Exp B; striped bars) each experiment is given as the mean of 100 scored comets on three replicate gels.

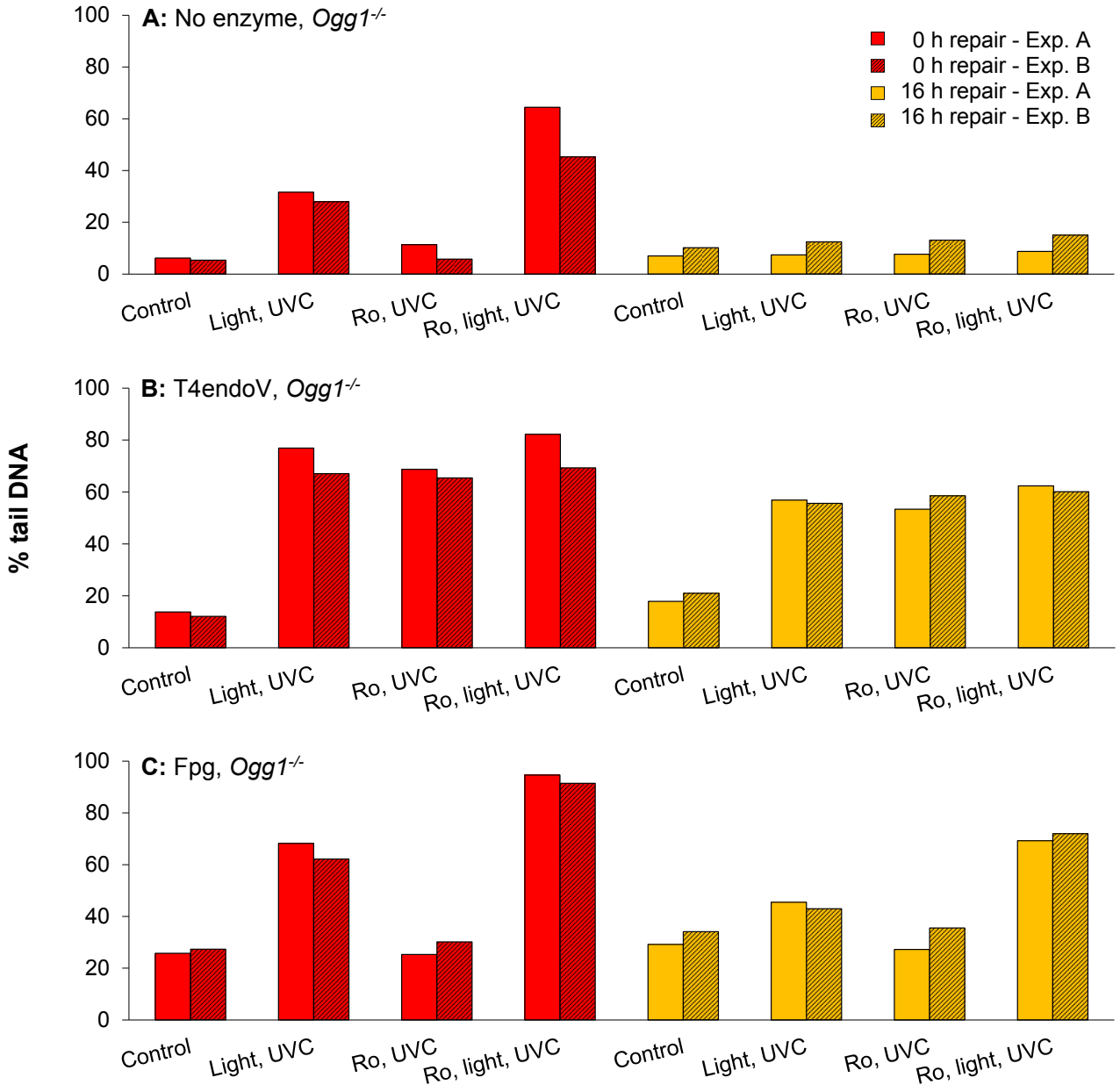

Figure A.2: DNA repair of UVC-induced DNA lesions in mouse embryonic fibroblasts (MEFs) from *Ogg1*$^{-/-}$ mice following a simultaneous single exposure to oxidative stress. DNA damage is measured in the comet assay in MEFs exposed to Ro 12-9786 (2 µm), light (12 min), and UVC (0.5 J/m^2), as indicated, before and after 16 h of repair. Tail DNA intensities (%) are presented of *Ogg1*$^{-/-}$ MEFs exposed to the following: Unexposed control; light and UVC; Ro and UVC; Ro, light and UVC, in the respective order. Gels were incubated without enzyme-extract (A), with T4endoV-extract (B) or with Fpg-extract (C). The MEFs were harvested immediately after exposure (red bars) or following 16 h repair (orange bars). Two experiments are shown (Exp. A; full bars, Exp B; striped bars), each experiment is given as the mean of 100 scored comets on three replicate gels.

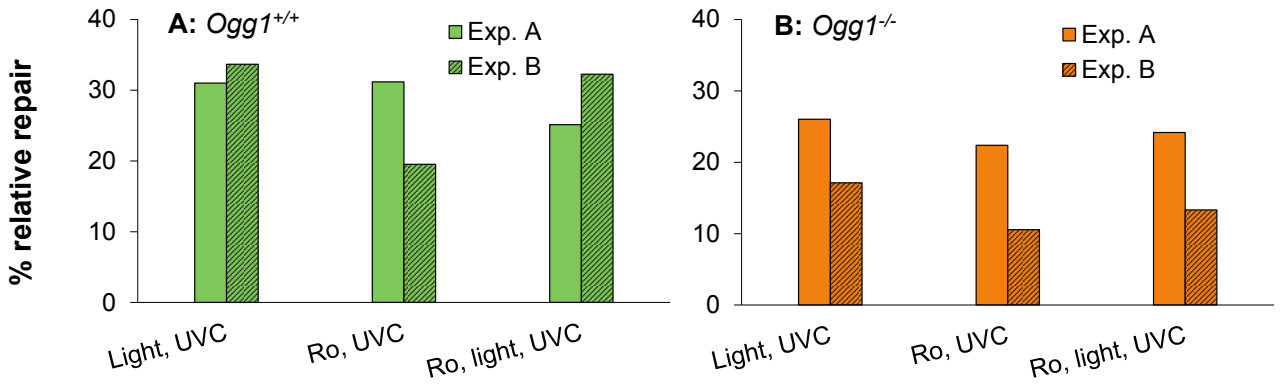

Figure A.3: Relative repair of T4endoV-sensitive sites and single strand breaks. MEFs from *Ogg1*$^{+/+}$ (A) or *Ogg1*$^{-/-}$ (B) mice were exposed to UVC (0.5 J/m^2), light (12 min) and Ro 12-9786 (2 µm), as indicated. DNA damage was measured before and after 16 h of repair and relative repair (%) was calculated. Two experiments are shown (Exp. A; full bars, Exp. B; striped bars).

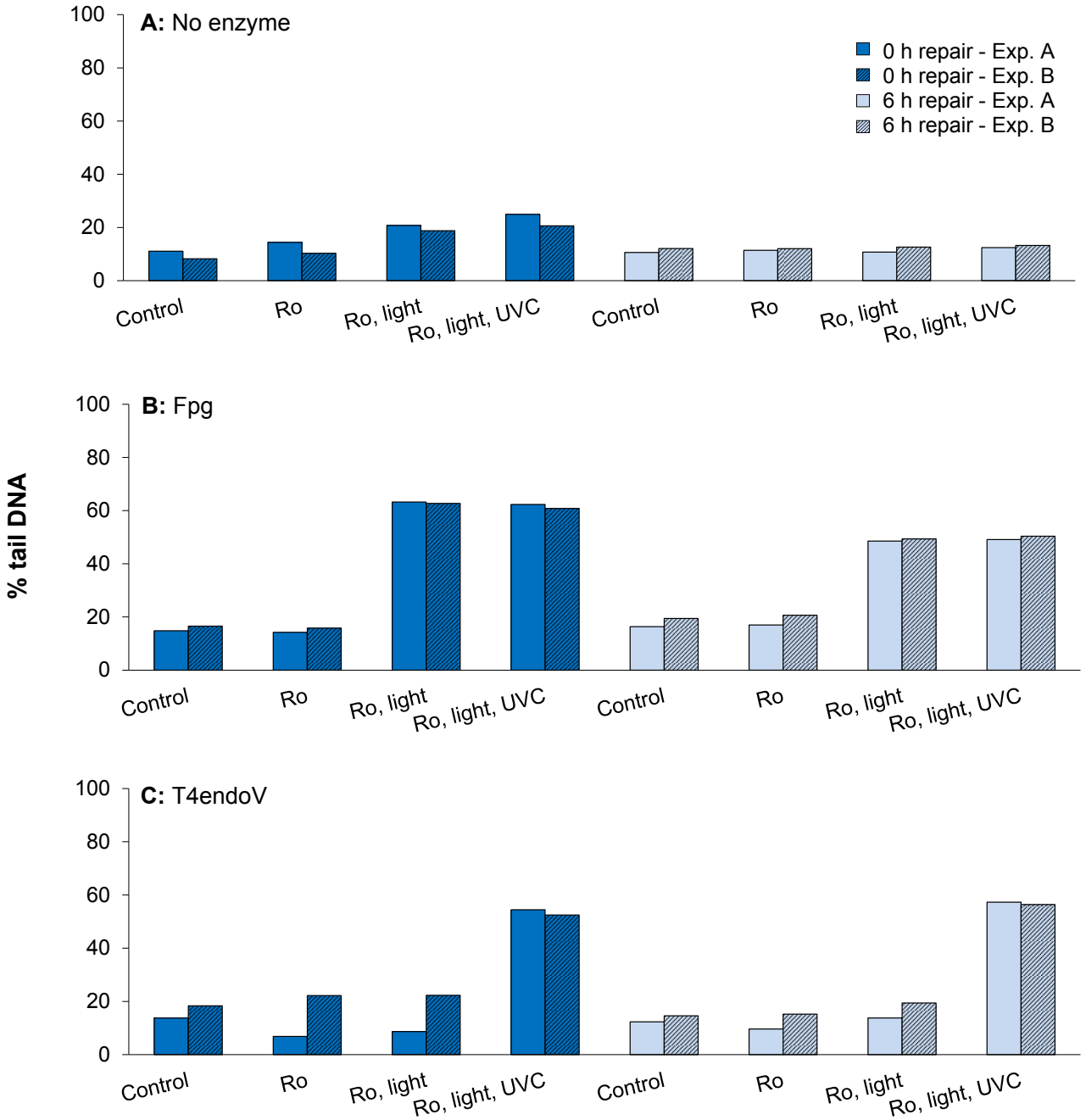

Figure A.4: DNA repair of oxidative DNA lesions in mouse embryonic fibroblasts (MEFs) from *Ogg1*$^{+/+}$ mice following a simultaneous single exposure to UVC. DNA damage is measured in the comet assay in MEFs exposed to Ro 12-9786 (2 µm), light (6 min), and UVC (0.5 J/m^2), as indicated, before and after 6 h of repair. Tail DNA intensities (%) are presented of *Ogg1*$^{+/+}$MEFs exposed to the following: Unexposed control; Ro; Ro and light; Ro, light and UVC, in the respective order. Gels were incubated without enzyme-extract (A), with Fpg-extract (B) or with T4endoV-extract (C). The MEFs were harvested immediately after exposure (dark blue bars) or following 6 h repair (light blue bars). Two experiments are shown (Exp. A; full bars, Exp B; striped bars), each experiment is given as the mean of 100 scored comets on three replicate gels.

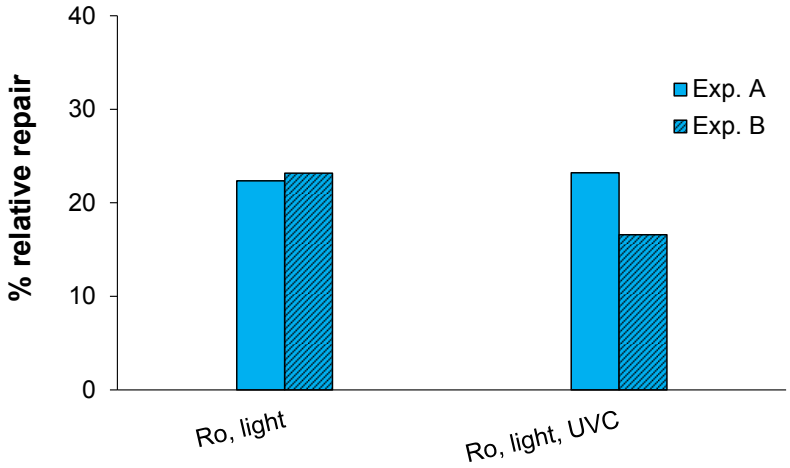

Figure A.5: Relative repair of Fpg-sensitive sites. MEFs from *Ogg1*$^{+/+}$ mice were exposed to Ro 12-9786 (2 µm), light (6 min), and UVC (0.5 J/m^2), as indicated. DNA damage was measured before and after 6 h of repair and relative repair (%) was calculated. Two experiments are shown (Exp. A; full bars, Exp. B; striped bars).

APPENDIX B

Solutions and media

0.75% Agarose solution (low melting point) for the comet assay

Added 0.075 g NuSieve GTG Low melting agarose to 10 ml of 10 mM EDTA-solution, warmed up to boiling point until the agarose was dissolved, and kept at 37 °C in a warming block.

10 mM EDTA-solution (for 0.75% Agarose solution) for the comet assay

1.86 g disodium EDTA (Na_2EDTA) was dissolved in 500 ml PBS without calcium and magnesium and pH was adjusted to 7.4 with sodium hydroxide (NaOH).

Lysis solution for the comet assay (stock)

2.5 M* sodium chloride (NaCl)

100 mM* EDTA

10 mM* tris(hydroxymethyl)aminomethane (tris-base)

1%* sodium lauryl sarcosinate (SLS)

Dissolved in dH_2O, before SLS was added pH was adjusted to 10 with NaOH pellets. When everything was dissolved, pH was adjusted again to 10 with concentrated HCl or 10 M NaOH.

*) This is stock solution, final concentration was achieved after addition of DMSO and Triton-X

Lysis solution for the comet assay (for four GelBond® films)

300 ml Lysis stock solution

10% DMSO

1% Triton-X

Neutralising buffer for the comet assay

0.4 M Tris-base

Dissolved in dH_2O and pH adjusted to 7.5 with concentrated HCl.

Electrophoresis buffer for the comet assay

10 M NaOH

200 mM EDTA

Dissolved in dH_2O and pH adjusted to 13.2 with concentrated HCl.

Enzyme reaction buffer for the comet assay

40 mM Hepes

0.1 M KCl

0.5 mM EDTA

Dissolved in dH_2O and pH adjusted to 7.6 with 7M KOH.

TE-buffer

1 mM EDTA

10 mM Tris-HCl

Dissolved in dH_2O and pH adjusted to 8.0.

Growth medium

500 ml bottle DMEM with 25 mM Hepes and 4.5 g/l Glucose

10 % non-heat inactivated FCS (50 ml)

2 % L-glutamine

1 % P/S.

1.2 mM Ro 12-9786 stock

6 mM Ro 12-9786 was diluted 1:5 in DMSO

APPENDIX C

Products and producers

Product	Producer	Country
A312f camera	Basler Vision Technologies	Germany
Absolutt alkohol prima (100 % (absolute) ethanol)	Arkus kjemi	Norway
Bio Whittaker® Dulbecco's Modified Eagle's Medium (DMEM)	Lonza	Belgium
BioWhittaker® Trypsin EDTA	Lonza	Belgium
Bovine serum albumin (BSA)	Sigma-Aldrich	USA
Centrifuge tube (15 ml)	Thermo Fisher Scientific/Nunc	USA
Comet assay IV (image analysis software)	Perceptive Instruments	UK
Costar® Traditional Straight Neck Cell Culture Flask with Phenolic-Style Cap (75 cm^2 and 162 cm^2)	Corning	USA
CryoTube™ (1.8 ml)	Thermo Fisher Scientific/Nunc	USA
Dimethyl sulphoxide (DMSO)	Merck	Germany

Ethyl 7-oxo-7h-thieno[2,3-A]-quinolizine-8-carboxylate (Ro 12-9786)	Roche	Switzerland
Ethylenediaminetetraacetic acid disodium salt dihydrate (EDTA-Na_2)	Sigma-Aldrich	USA
Foetal calf serum (FCS) (non-heat inactivated)	Gibco	USA
Formamidopyrimidine DNA glycosylase (Fpg)-extract	Locally produced	Norway
GelBond® Film	Cambrex	USA
Halogen light (500 W)	Femco	USA
Hepes	Sigma-Aldrich	USA
Hydrogen chloride (HCl)	Merck	Germany
L-glutamine	Sigma-Aldrich	USA
Lymphoprep™ tube	Axis-Shield PoC	Norway
Mercury Short-Arc HBO® 100 W/2 lamp	Osram	Germany
NuSieve GTG Low Melting Agarose	Cambrex	USA
Olympus Burner	Olympus	Japan
Olympus BX51 microscope	Olympus	Japan
Penicillin/Streptomycin	PAA Laboratories GmbH	Austria
Phosphate buffered saline (PBS)	Locally produced	Norway

Potassium chloride (KCl)	Merck	Germany
Potassium dihydrogenphosphate (KH_2PO_4)	Merck	Germany
Potassium hydroxide (KOH)	Merck	Germany
RIDA®FLUOR *Mycoplasma* IFA immunofluorescence assay	R-Biopharm AG	Germany
Sodium chloride (NaCl)	Merck	Germany
Sodium hydrogenphosphate (Na_2HPO_4)	Merck	Germany
Sodium Hydroxide (NaOH)	Merck	Germany
Sodium lauryl sarcosinate (SLS)	Sigma-Aldrich	USA
Sterile water	Fresenius	Germany
SYBR® Gold	Invitrogen	USA
T4 endonuclease V (T4endoV)-extract	Locally produced	Norway
TC-Treated Culture Dish (35mm)	Corning	USA
Trisma® HCl	Sigma-Aldrich	USA
Triton-X	Sigma-Aldrich	USA
Trizma® base	Sigma-Aldrich	USA
Trypan Blue	Sigma-Aldrich	USA